Defense Documentation Center

Defense Supply Agency

Cameron Station • Alexandria, Virginia

NOTICE: THIS DOCUMENT CONTAINS INFORMATION AFFECTING THE NATIONAL DEFENSE OF THE UNITED STATES WITHIN THE MEANING OF THE ESPIONAGE LAWS, TITLE 18, U.S.C., SECTIONS 793 and 794. THE TRANSMISSION OR THE REVELATION OF ITS CONTENTS IN ANY MANNER TO AN UNAUTHORIZED PERSON IS PROHIBITED BY LAW.

[redacted]
SECURITY INFORMATION

NRL MEMORANDUM REPORT No. 164

QUANTITATIVE MEASUREMENTS OF RADAR ECHOES FROM AIRCRAFT XI. B-29

W. S. Ament
F. C. MacDonald
H. J. Passerini

RADIO DIVISION I

25 May 1953

NAVAL RESEARCH LABORATORY, WASHINGTON, D.C.

[redacted]

[redacted] SECURITY INFORMATION

(6)

QUANTITATIVE MEASUREMENTS OF RADAR ECHOES FROM AIRCRAFT.

XI. B-29.

(9) Memorandum rept.

By

(10) W. S. Ament,
F. C. MacDonald
H. J. Passerini

(11) 25 May [redacted]53 (12) 48 p.

Wave Propagation Research Branch
Radio Division I
Naval Research Laboratory
Washington 25, D. C.

(251950)

[redacted]

(14) NRL-MR-164

NM-

DISTRIBUTION

ANAF/GM Mailing List	43
CNO	
Attn: Op-03D	1
Attn: Op-05	1
Attn: Op-42	1
Attn: Op-342E	1
Attn: Op-374	1
ONR	
Attn: Code 427	1
Attn: Code 459	1
Attn: Code 470	1
BuAer	
Attn: El 80	1
BuOrd	
Attn: Re4f	1
BuShips	
Attn: Code 801	1
Attn: Code 820	1
Attn: Code 835	1
ComOpDevFor	1
WSEG	2
CO and DIR., USNEL	2
OCSigO	
Attn: Ch., Eng. and Tech. Div. SIGTM-S	1
CO, SCEL	
Attn: Dir. of Eng.	2
CO, Rome Air Dev. Center - Griffis A.F.B., Rome, N. Y.	
Attn: ENR	1
CO, Air Force Cambridge Res. Labs	
Attn: ERRS	1
Dir., NBS	
Attn: CRPL	1

[redacted]

RDB	
Attn: Information Requirements Branch	2
Attn: Navy Secretary	1
Attn: Committee on Electronics (Secretariat) For further distribution to: Panel on Antennas and Propagation, and Subpanel on Radar Reflection Characteristics	30
BJSM (Navy Staff)	1
BJSM (Army Staff)	1
BJSM (Air Staff)	1
Canadian Joint Staff Attn: Navy Member	5
Australian Joint Service Staff	5
ASRE, England	1
DRE, Admiralty, England	1
Ministry of Supply, England	1
RRDE, England	1
TRE, England	1

[redacted]
SECURITY INFORMATION

[redacted]

ABSTRACT

B-29 echo amplitudes, sampled over 10 second intervals, are found to be approximately Rayleigh distributed at X band, less so at S band, and least at L band. At broadside aspect and normal to the leading edge of the wing, the L-band echo is steadier than a Rayleigh distributed echo; at many other aspects, the propeller modulation causes the L-band echo to fluctuate through a greater range than would a Rayleigh distributed echo. The same tendency is found to a lesser degree at S band, and to a slight degree at X band.

The average radar areas are found to be 103, 370 and 75 square meters for L, S, and X bands respectively. No theoretical reason can be advanced to explain why the S-band average should be so much larger than the L- and X-band averages; it appears likely that the difference may be due to a systematic experimental error.

The frequency spectrums of echo amplitude are found to contain sharp components due to propeller modulation, and possibly also to vibration of parts of the aircraft's surface. At spectral frequencies lower than these beat notes, components are found whose frequency is roughly proportional to radar frequency, suggesting that they are produced by the variations of phase between the echoes from different parts of the aircraft.

[redacted]
SECURITY INFORMATION

PROBLEM STATUS

This is an interim report on the problem; work continues.

AUTHORIZATION

NRL Problem R11-17
WADC CSO No. 52-849

INTRODUCTION

In ten previous reports,(1)-(10) characteristics of radar echoes from various aircraft were given. This report, the eleventh of the series, gives the complete results obtained for the B-29. The measurements on the B-29 were taken during two days of operation. Neither of the two operating days gave a complete set of data on the B-29, so that the results were derived from a combination of L- and S-band data from one day, and L- and X-band data from the other day.

Amplitude Distributions

The amplitude distributions plotted in Figs. 2 - 10 are representative 10-second (1200 pulse) samples of the airplane aspects (defined in Fig. 1) encountered. In these figures, cumulative distributions of echo pulse amplitudes are plotted, the ordinate being $10 \log_{10} \sigma$ (σ = radar area in square meters), the abscissa being the percent of time the amplitude of the observed echo exceeds the ordinate. For comparison, a straight line is drawn with the same slope as the theoretical cumulative distribution (Rayleigh distribution) of noise powers.

On the various plots, points indicated by ⊡, ⊙ and ⧋, represent X-, S-, and L-band observations, respectively. Thus, distributions plotted against a single ordinate scale represent simultaneous observations, at two differing radar frequencies, of the distribution of radar areas, the intention being to emphasize differences between the radar area distributions.

In the main, the distributions tend to fit the theoretical Rayleigh distribution better as the radar frequency increases. Deviations from the Rayleigh distribution will now be discussed with reference to the L-band data. The L-band distributions can be fairly well fitted with straight lines, either having steeper slopes than the Rayleigh line (as in Fig. 3, bottom, Fig. 5, bottom, Fig. 7, bottom, and Fig. 10, bottom) or with less steep slopes than the Rayleigh line (as in Figs. 2, 3 top, 8 top). To a lesser degree, the same general tendencies are found in the corresponding S- and X-band plots; the S-band run of Fig. 2 seems to be an exception.

On the L-band pulse-to-pulse films sampled in preparation of the plots which show steep slopes, there was strong propeller modulation The pulse-by-pulse record approximately corresponding to Fig. 3, bottom, is found transcribed in Fig. 22c. For the single-engined F-51, the propeller modulation was shown (in Report IX) to raise the level of the stronger echoes well above the Rayleigh line fitted to the weaker echoes. The effect was quite sharp for the F-51, owing to the regularity with which propeller echoes appeared in the filmed records. The B-29 carries four propellers which are only approximately synchronized, so that the strong echoes attributable to the propellers are neither so regularly spaced in time, nor so consistently strong relative to the remainder echoes, as was the case with the F-51. (Compare, for instance, the pulse-to-pulse voltage plots in Fig. 18, Report IX, with those of the present

Fig. 24; the azimuths are about the same in the two Figures.)

Finally, the percentage of B-29 echoes affected by one or more of the four propellers is larger than the percentage of F-51 echoes affected by its single propeller. This statement is based on the assumption that most of the strong, sharp echoes in the pulse-by-pulse voltage plots referred to are attributable to propeller effects; the assumption is based on a comparison of these plots with the much smoother pulse-by-pulse voltage plots produced by the propellerless B-45 (Report VIII, Figs. 21, 22, 23). In sum, propeller-affected echoes appear both more frequently and with a greater amplitude range for the B-29 than for the F-51. Thus, in B-29 echo amplitude distributions, the propeller-affected echoes occupy a larger percentage of the total distribution, and the gradation in power levels among the various percentages should be more continuous than for the F-51. Qualitatively, then, the B-29 propeller-affected distributions should be smoothed-out versions of the corresponding F-51 distributions, as is observed.

The L-band echo power distributions with slopes less steep than that of the theoretical line are found at azimuths about ±7°(Figs. 2, top, and 3, top) and near broadside (azimuth 91°-96°, Fig. 8, top). The B-29 wing has a listed 7°1' sweepback, so that strong echoes from the leading edge of the wing may be expected at approximately this azimuth. Near broadside aspect, of course, the echo from the fuselage is relatively great, and any propeller modulation is reduced to a relative ripple,

especially since the blades are viewed more or less edgewise. The relatively small propeller modulation at broadside aspect is observable in the pulse-by-pulse plot of Fig. 23a, and more pronounced propeller modulation occurs in Fig. 22c near the leading edge aspect. For these aspects the echo is dominated by a more or less steady reflection from a single portion of the surface, and has the general characteristics of the echo from a propellerless plane. In such situations the slope of the distribution depends basically on the number of lobes of the radar reflection pattern that are observed in the sampled 10 seconds. As explained in Report VIII, the number of such lobes increases with radar frequency, so that the X-band echoes have a greater tendency to be Rayleigh distributed than the L-band echoes.

A special case of these effects is illustrated by the distributions of Fig. 3. The two sets of distributions shown there result from data obtained on two different flights (on different days) for which the listed azimuths are almost identical. Yet the two sets of distributions are different, the ones at the top being less steep, and the ones at the bottom steeper than the Rayleigh distribution. From the corresponding range plots (Figs. 13 and 19, respectively) it can be seen that these samples each contain a high-amplitude, low-frequency component, which serrates the regular ground reflection interference lobe on L band. For the flight corresponding to Fig. 13, the change of average azimuth was fairly regular during the 10 seconds of the sample, and amounted to about

0.2 degrees. The low-frequency components are simultaneous on both L and S bands in this sample, so that this sample quite definitely contains the echo from the leading edge of the wing. Since the leading edge echo is large relative to the other contributions in this aspect region, it is dominant, and thus results in a compression of the range of amplitude fluctuation during the sample. The distribution therefore has a smaller slope than the Rayleigh distribution. For the flight corresponding to Fig. 19, however, the change of average azimuth was almost zero. The average aspect hovered near a constant value, with the dynamic variations due to flight conditions superimposed on this constant value. From the X-band plot of Fig. 19, it can be seen that flashes of the leading edge echo occur between ranges of about 35,900 and 37,200 yards (on L band the strongest flash rises sufficiently above the minimum of the ground reflection interference lobe to be just observable). The sample from which the lower set of distributions of Fig. 3 was prepared, however, corresponds to ranges of 38,400 to 39,300 yards. Thus it is evident that for this sample the average aspect was not centered on the leading edge, but that the dynamic variations of aspect swept briefly into part of the leading edge lobe. These brief "flashes" of strong amplitude would result in a greater range of amplitude fluctuation than normal, so that the distribution would have a steeper slope than the Rayleigh distribution. In further support of this explanation, the median level of the upper distribution is higher (approximately 15 decibels) than that

of the lower distribution.

In summary, the B-29 radar echo, sampled over a ten second period, is approximately Rayleigh distributed when neither the propellers nor a single, strongly echoing surface of the airplane produces the majority of strong echoes in the sample. When the propellers are dominant, the echo shows a greater range of fluctuation than would a Rayleigh distributed echo, because the strong propeller echoes occur only during the relatively small percentage of time when the blades are favorably oriented. When the strongest echoes in the sample arise from a single favorably oriented surface of the B-29, (such as the fuselage or the leading edge of the wing) the echo distribution shows a greater average fluctuation range than in the Rayleigh distribution when the dominant echo flashes into the radar only once or twice during the ten seconds, and shows a lesser average fluctuation range (and stronger mean echo power) when the dominant echo is observed throughout the time of the sample.

Aspect Dependence

Each of Figs. 11 - 19 covers one flight of the aircraft, and consists of three graphs. The uppermost graph of each figure consists of a plot of the aircraft's aspect, as defined in Fig. 1, versus range in thousands of yards. The remaining two graphs of each figure consist of plots of radar area versus range in thousands of yards. Each graph consists of three sets of points, each set being connected by straight line segments. Each point represents about one second of data, and data taken

simultaneously are aligned vertically so that the uppermost point in each graph is the maximum, the middle point is the median, and the lowest point is the minimum radar area occurring in that second. The radar area as plotted contains variations due to interference lobes caused by ground reflections. At the center of each lobe, or integral number of lobes, is a circled x (⊗) indicating the median value (reduced to "free-space" value in accordance with the procedure described in the Appendix to (2)) of the 1-second median radar area values for that lobe or integral number of lobes, and these median values were used in determining the median value of σ for each five degrees of azimuth as described below.

At the bottom of each plot, the step-like curve gives the radar area, in 1 db increments, of a target just detectable by the radar at the particular range (neglecting the receiver recovery time characteristic). Therefore, it really represents minimum detectable area only at ranges beyond receiver recovery.

The data were divided into intervals, each of which spanned five degrees of azimuth. For each such interval the median of the one-second median points was determined for each frequency. These "median-median" values are plotted in Fig. 20.

The target azimuth, as calculated from the recorded azimuth of the optically pointed radar and the true heading assigned to the B-29 for the particular run, was not concordant with the azimuth determined from the positions of the broadside echo and the echo from the leading edge of

the wing (7° sweepback). The difference amounted to as much as 8°, which is about what would be expected if the B-29 had flown magnetic headings, rather than the specified true headings. The azimuth angles, therefore, have been changed to agree with the expected positions of the leading edge and broadside echoes.

Frequency Dependence

To obtain representative measures of the radar area of the B-29, the following procedure was carried out for each radar frequency employed. From Fig. 20, a single number for the radar area was obtained on each frequency for each five-degree azimuth interval by averaging all the "median-median" areas (in square meters) in that azimuth interval, without regard to elevation angles involved. The results are plotted in Fig. 21. The following two estimates of the average radar area of the B-29 were then obtained, using the "average-median-median" data of Fig. 21. In the first estimate, the Fig. 21 data at each frequency were averaged (in square meters) over the 19 five-degree intervals containing data on all three frequencies.

	L	S	X
Square meters	103.3	370.2	74.8
db > 1 m^2	20.1	25.7	18.7

A second estimate was obtained by calculating, for each frequency, the average (in square meters) of all the "average median-median" radar areas plotted in Fig. 21.

	L	S	X
Square meters	94.6	334.1	66.9
db > 1 m^2	19.8	25.2	18.3

The trend with radar frequency indicated in the above tables has no theoretical explanations known to the authors. It cannot be attributed to the particular aspects averaged because the trend is found, for example, in each L- and S-band entry in over more than 90° of azimuth; nor can it be attributed to using median rather than average values, because the S- and L-band distributions of echo amplitudes do not differ sufficiently. In view of these features, the difference must be systematic, so that it represents either a real difference of radar area with frequency or a systematic experimental error. Since the shapes of the curves of Fig. 21 are rather closely similar for all three frequencies, it appears more likely that the high S-band value is due to a systematic experimental error.

Fluctuations of the B-29 Echo

Spectrums of selected 5-second samples of B-29 echoes were prepared according to the procedure described in Report VII. The necessary plots of video voltage versus time are shown in Figs. 22 - 24, and the spectrums for aspects near head-on, near broadside, and toward the tail are shown in Fig. 25 - 27 respectively. Following the method described in Report IX, the spectrums are also plotted against an expanded frequency scale in Figs. 28 - 30.

For nearly head-on aspects (Figs. 25 and 28), and for the 'tailward' aspect interval (Figs. 27 and 30), the dominant frequencies of the

spectrums are the frequencies arising from beating between the propeller echoes and the pulse repetition frequency, in the manner discussed in Report IX. The stronger beat frequencies are found at about 47 and 27 cps in Figs. 25 and 27, with 7 and 14 cps beat frequencies being most in evidence at L band and least at X band in these plots.

For a B-29 at cruising speed, the nominal rotation rate of the propellers is 2400 rpm. The propellers have four blades, so that the same aspect of a propeller is presented to the radar each 90° of rotation, or 160 times per second. The beat between this 160 cps periodicity and the 120 cps pulse repetition frequency of the radar would lead to a 40 cps component of modulation in the echo. For the observed 47 cps modulation frequency, the required propeller-aspect periodicity is 167 times per second, corresponding to a propeller rotation rate of 2505 rpm, which is a reasonable value.

Additional beats between the various harmonics of 167 cps present in the modulation envelope and the harmonics of the 120 cps pulse repetition frequency are possible in the video output. This can be explained in the following way:

If the B-29 had been observed with a c-w radar, the propeller modulation would have appeared as a complicated periodic wave with fundamental frequency about 167 cps. If this wave were subjected to a spectral analysis, harmonics of 167 cps would appear to some degree, depending on the complication of the continuous periodic wave form; in other words, a c-w record

of the propeller echo might contain the frequencies 2x167 = 334 cps, 3x167 = 501 cps, etc.. Now the radar pulsed at 120 cps samples this hypothetical record at discrete, evenly spaced points. A spectral analysis of a long series of radar pulses would show the fundamental 120 cps pulse repetition frequency, plus all of its harmonics, with substantially the same power in each of the lower harmonics as is found in the fundamental. That is, an analysis of the periodic radar pulse envelope would contain frequency components at 120, 240, 360, 480, nx120 cps, all having about equal power. The pulse-to-pulse sample recorded on the films is essentially the result of mixing the envelope of the c-w B-29 echo with the periodic radar pulse envelope, and rectifying the result. Hence the pulse-by-pulse record contains the difference frequencies, or beats, between each harmonic of the pulse repetition frequency and each harmonic present in the envelope of the c-w echo from the airplane. With the 47 cps beat frequency regarded then as the difference between the two fundamentals, 120 cps and 167 cps, the record may well contain the beat frequencies 3x120 - 2x167 = 26 cps, 4x120 - 3x167 = 21 cps, etc. Sum frequencies would also be found in the record, but would not be displayed by the present spectrums, which are confined to frequencies below 60 cps. Many difference frequencies other than those listed are also too high to be displayed.

Detailed examination of the spectrums shows that many of the spectrum lines can be identified as being generated by propeller modulation. Many

other lines of the same fluctuation frequency are found on different radar frequencies. These fluctuation frequencies cannot be attributed to the propellers in the foregoing manner, so that some other mechanism must be sought to explain why these fluctuation frequencies appear independent of radar frequency. A possible mechanism may lie in mechanical vibrations of the aircraft's surface.

Although the propeller echo is relatively weak at broadside aspect, traces of the 47- and 27-cps beat frequencies are to be found in the broadside spectrums of Fig. 26. The dominant spectral components at broadside are found in the low-frequency region, significantly below about 3, 4.5, and 8 cps on L, S and X bands, respectively. The expanded plot of Fig. 29 shows this in better detail than Fig. 26. This increase in significant fluctuation frequencies with radar frequency, is in general accord with the theory of aircraft echo fluctuations given in Report VIII, where the fluctuations (aside from propeller and vibration effects) were ascribed to beating of echoes from various portions of the aircraft. Analogous bands of low-frequency fluctuations are found in Figs. 28 and 30. Grossly speaking, these frequency bands have upper frequency limits which are proportional to radar frequency.

For the broadside aspect, this conclusion is perhaps more strikingly apparent in the pulse-by-pulse voltage plots of Fig. 23 than in the broadside spectrums. In Fig. 23, the general echo fluctuates at a rate about proportional to frequency, while the finer-grained fluctuation of the

echo is clearly the residual effect of propeller and vibration modulation.

Conclusions

B-29 echo amplitudes, sampled over 10 second intervals, are found to be approximately Rayleigh distributed at X band, less so at S band, and least at L band. At broadside aspect and normal to the leading edge of the wing, the L-band echo is steadier than a Rayleigh distributed echo; at many other aspects, the propeller modulation causes the L-band echo to fluctuate through a greater range than would a Rayleigh distributed echo. The same tendency is found to a lesser degree at S-band, and to a slight degree at X band.

The average radar areas are found to be 103, 370, and 75 square meters for L, S and X bands respectively. No theoretical reason can be advanced to explain why the S-band average should be so much larger than the L- and X-band averages; it appears likely that the difference may be due to a systematic experimental error.

The frequency spectrums of echo amplitude are found to contain sharp components due to propeller modulation, and possibly also to vibration of parts of the aircraft's surface. At spectral frequencies lower than these beat notes, components are found whose frequency is roughly proportional to radar frequency, suggesting that they are produced by the variations of phase between the echoes from different parts of the aircraft.

References

1) "Quantitative Measurements of Radar Echoes from Aircraft, I. B-36, B-45, F-51, and F-86," NRL Letter Report, Serial C-3460-73A/50 date 24 October 1950.

2) "Quantitative Measurements of Radar Echoes from Aircraft, II. Formation of three F-86's, B-29, F-80 with wing tanks, and F-80 without wing tanks," NRL Letter Report, Serial C-3460-18A/51 dated 12 February 1951.

3) "Quantitative Measurements of Radar Echoes from Aircraft, III. B-36 Amplitude Distributions and Aspect Dependence," NRL Letter Report, Serial C-3460-94A/51 dated 19 June 1951.

4) "Quantitative Measurements of Radar Echoes from Aircraft, IV. F-86 Amplitude Distributions and Aspect Dependence," NRL Letter Report, Serial C-3460-138A/51 dated 5 September 1951.

5) "Quantitative Measurements of Radar Echoes from Aircraft, V. Correction of X-band Values," NRL Letter Report, Serial C-3460-132A/52 dated 24 October 1952.

6) "Quantitative Measurements of Radar Echoes from Aircraft, VI. Corrected F-86 Amplitude Distributions and Aspect Dependance," NRL Letter Report, Serial C-3460-143A/52 dated 15 December 1952.

7) "Quantitative Measurements of Radar Echoes from Aircraft, VII. B-36 and F-86 Spectrums," NRL Memorandum Report No. 107 dated 15 January 1953.

8) "Quantitative Measurements of Radar Echoes from Aircraft, VIII. B-45," NRL Memorandum Report No. 116 dated 28 January 1953.

9) "Quantitative Measurements of Radar Echoes from Aircraft, IX. F-51 " NRL Memorandum Report No. 127 dated 4 March 1953.

10) "Quantitative Measurements of Radar Echoes from Aircraft, X. Three F-86 Aircraft in Formation," NRL Memorandum Report No. 144 dated 6 April 1953.

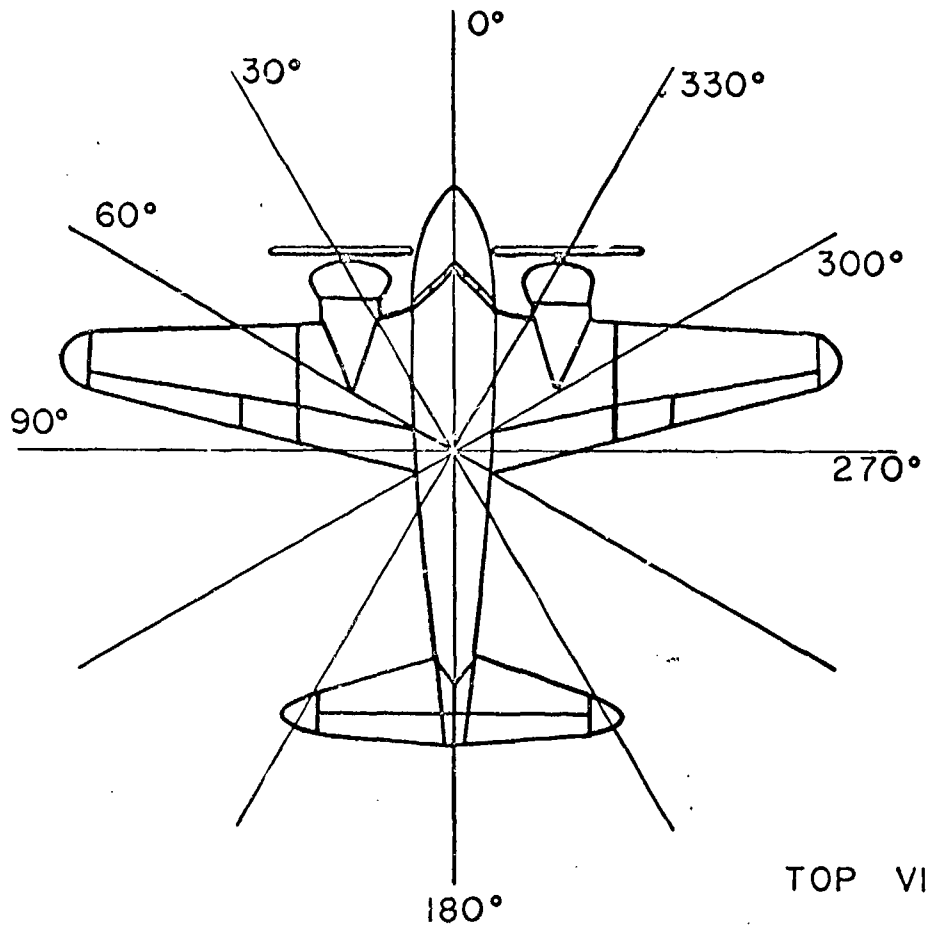

TOP VIEW

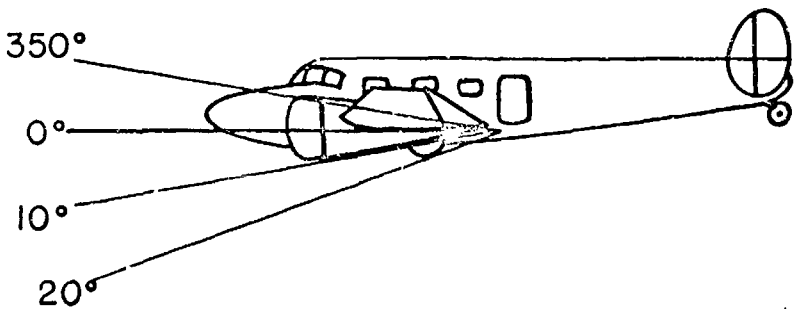

Definition of aspect angles

Figure 1

CONFIDENTIAL

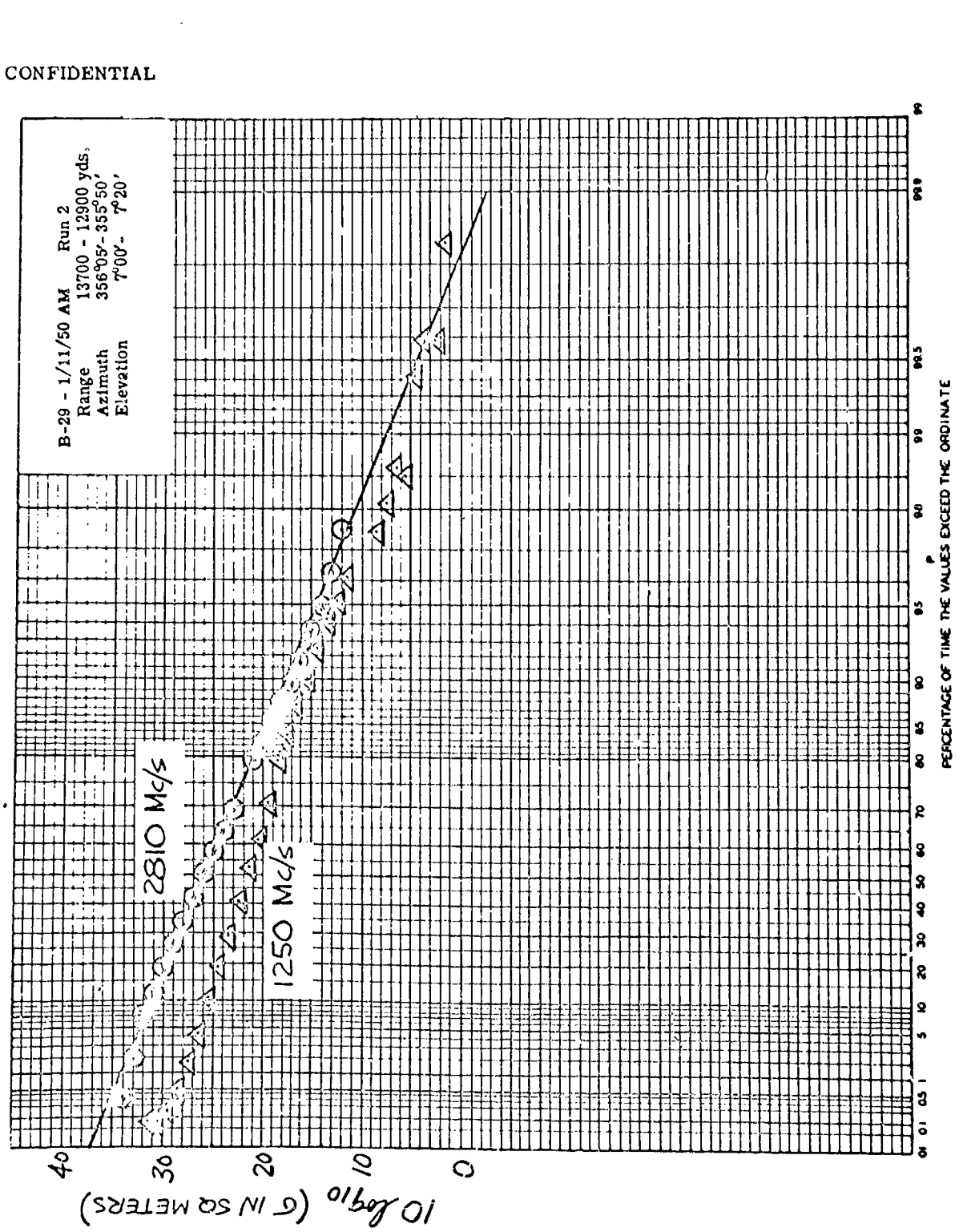

CONFIDENTIAL
SECURITY INFORMATION

Figure 2

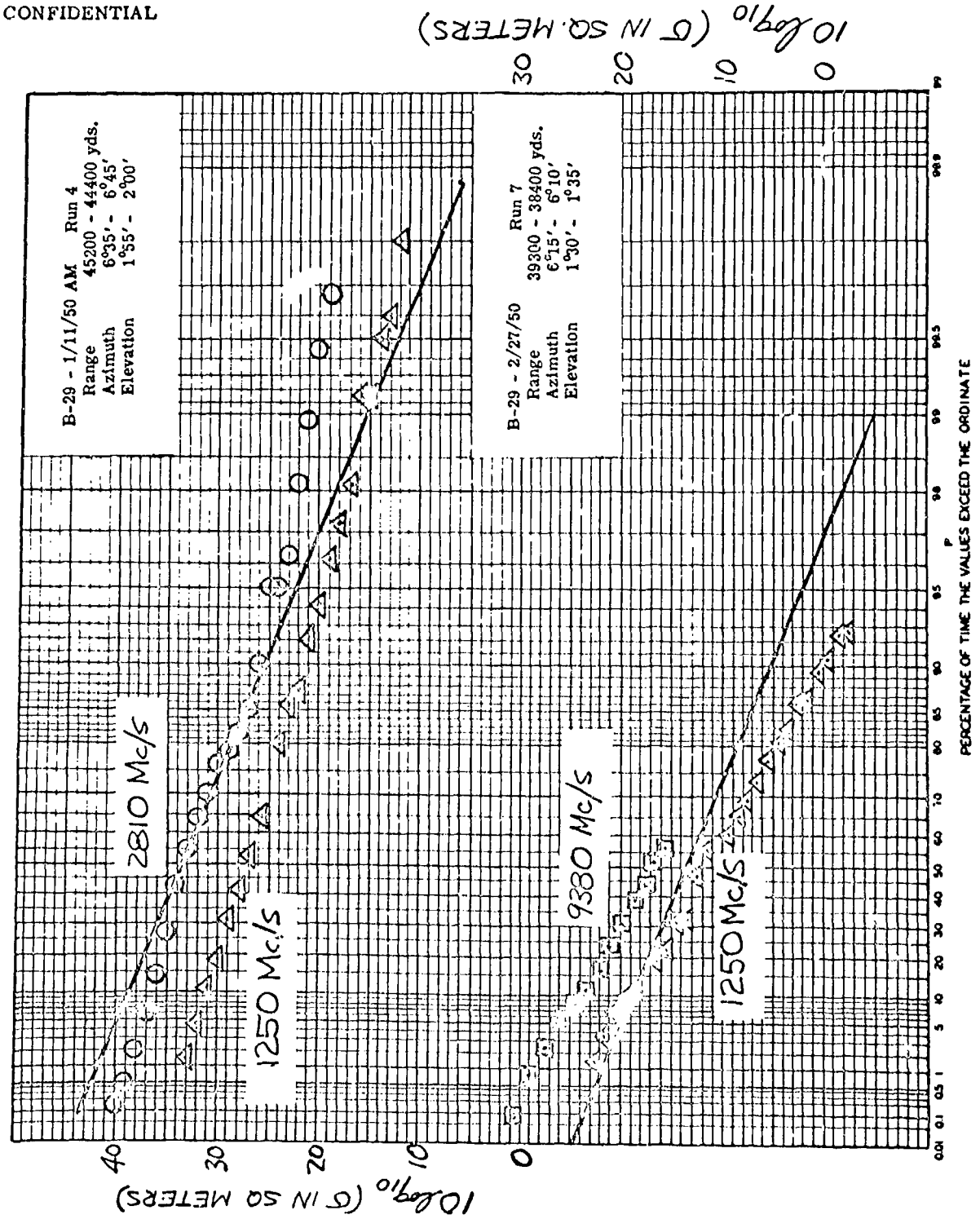
B-29 - 1/11/50 AM Run 4
Range 45200 - 44400 yds.
Azimuth 6°35' - 6°45'
Elevation 1°55' - 2°00'
B-29 - 2/27/50 Run 7
Range 39300 - 38400 yds.
Azimuth 6°15' - 6°10'
Elevation 1°30' - 1°35'
2810 Mc/s
1250 Mc/s
9380 Mc/s
1250 Mc/s
10 log10 (σ IN SQ. METERS)
PERCENTAGE OF TIME THE VALUES EXCEED THE ORDINATE

Figure 3

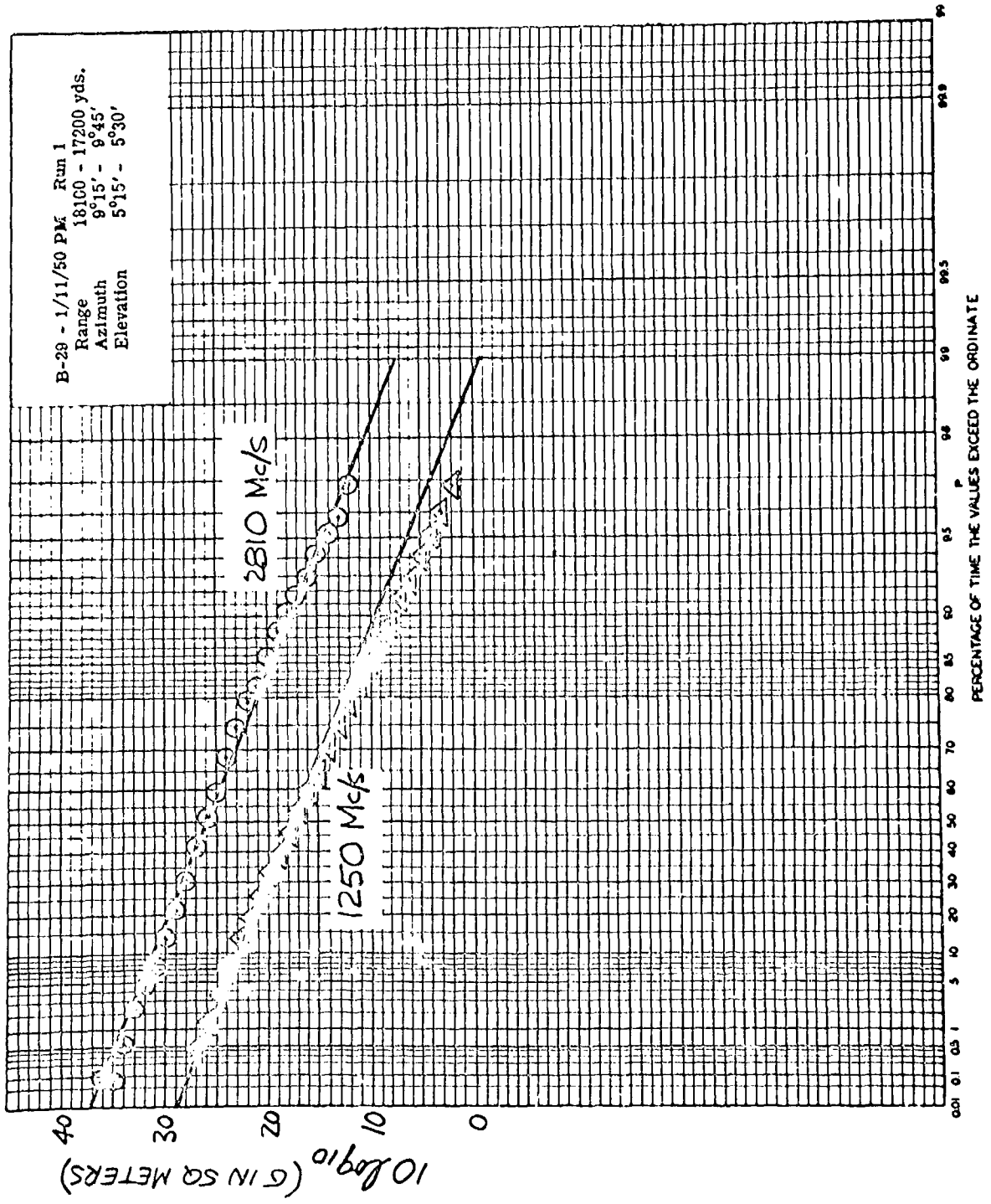
B-29 - 1/11/50 PM Run 1
Range 18100 - 17200 yds.
Azimuth 9°15' - 9°45'
Elevation 5°15' - 5°30'
2810 Mc/s
1250 Mc/s
10 log10 (σ IN SQ METERS)
40
30
20
10
0
PERCENTAGE OF TIME THE VALUES EXCEED THE ORDINATE
99.9
99.5
99
98
95
90
80
70
60
50
40
30
20
10
5
3
1
0.3
0.1
0.01

Figure 4

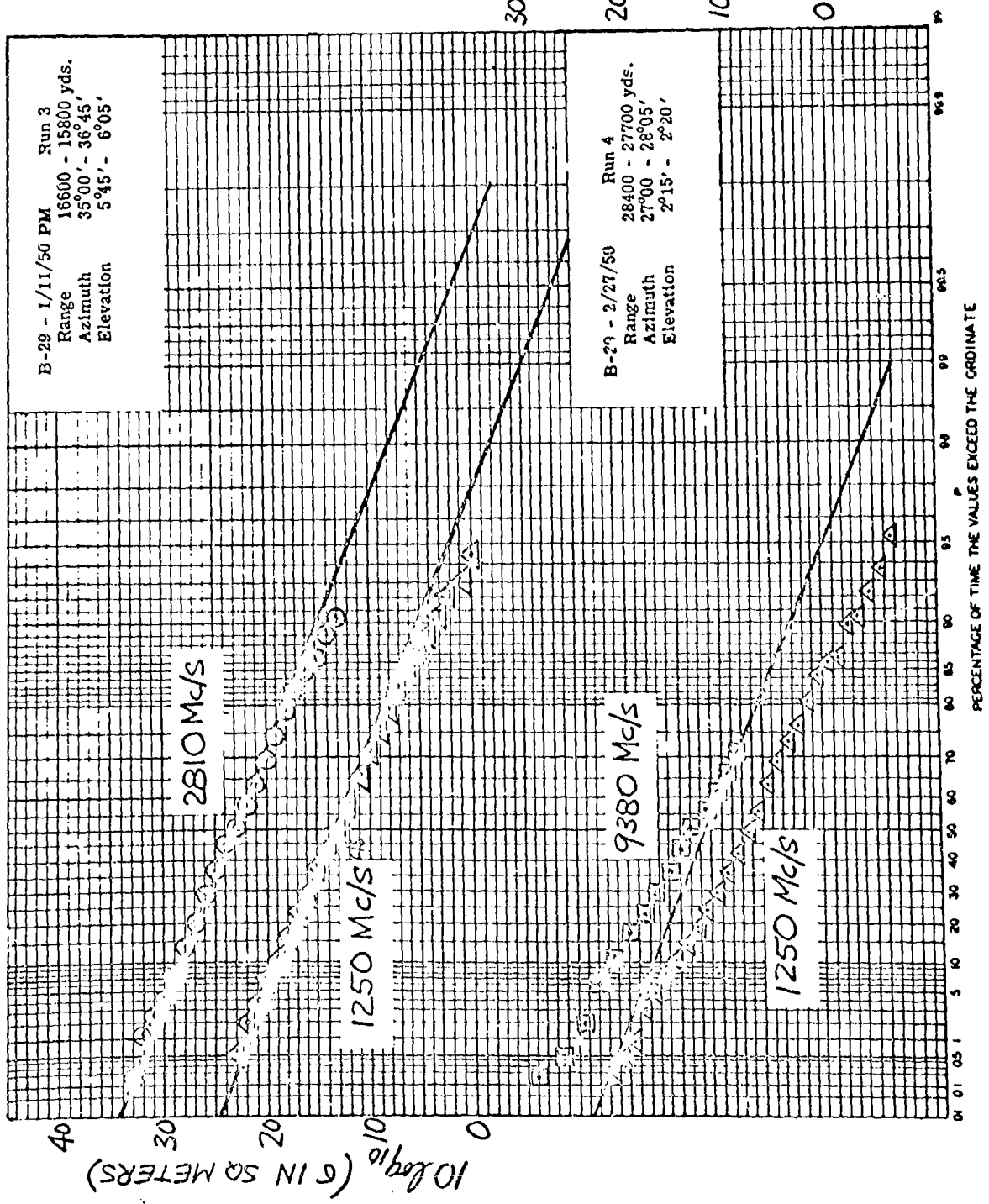
B-29 - 1/11/50 PM Run 3
Range 16600 - 15800 yds.
Azimuth 35°00' - 36°45'
Elevation 5°45' - 6°05'
B-29 - 2/27/50 Run 4
Range 28400 - 27700 yds.
Azimuth 27°00 - 28°05'
Elevation 2°15' - 2°20'
2810 Mc/s
1250 Mc/s
9380 Mc/s
1250 Mc/s
10 log10 (σ IN SQ METERS)
10 log10 (σ IN SQ METERS)
PERCENTAGE OF TIME THE VALUES EXCEED THE ORDINATE

Figure 5

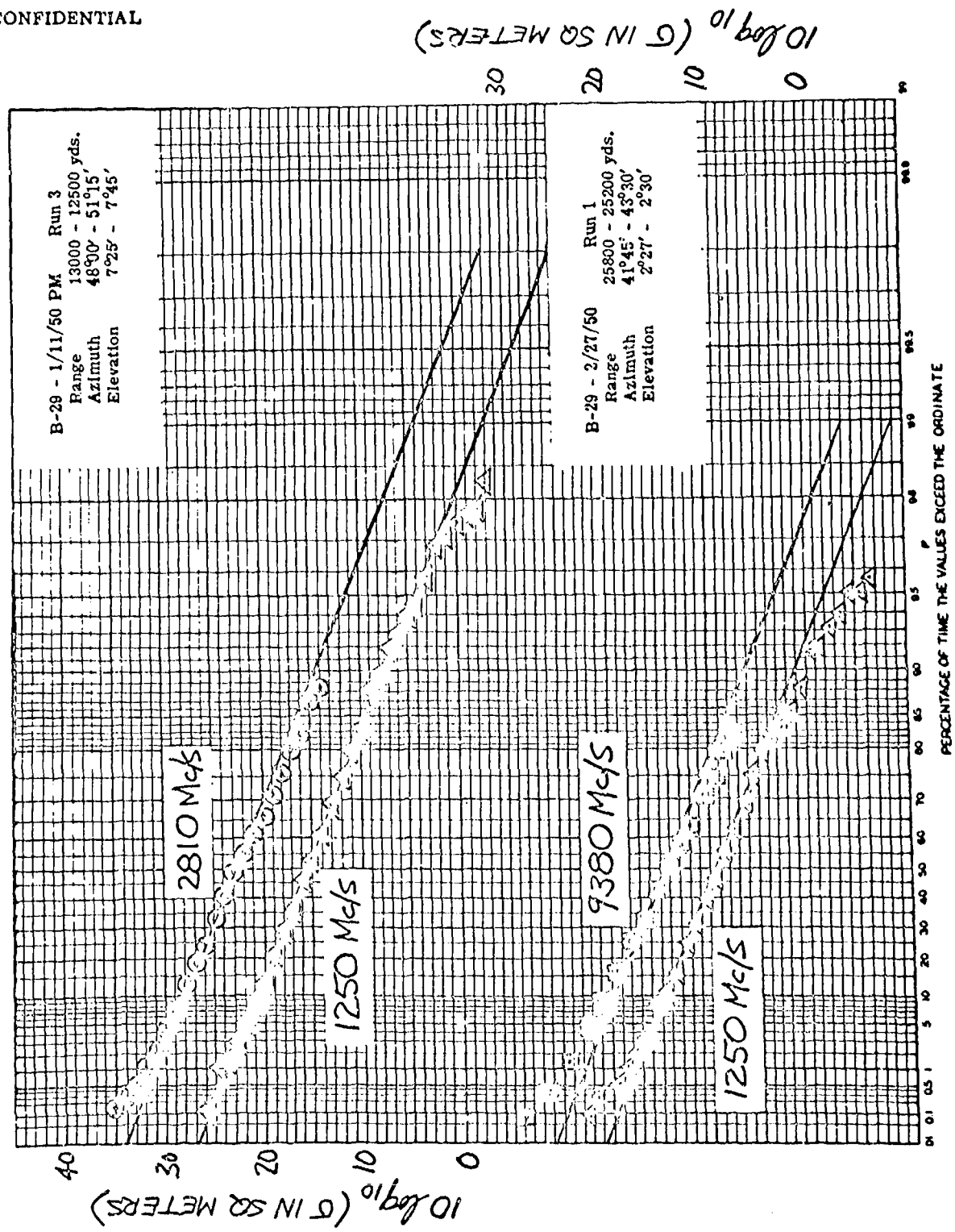
B-29 - 1/11/50 PM Run 3
Range 13000 - 12500 yds.
Azimuth 48°0' - 51°15'
Elevation 7°25' - 7°45'
B-29 - 2/27/50 Run 1
Range 25800 - 25200 yds.
Azimuth 41°45' - 43°30'
Elevation 2°27' - 2°30'
2810 Mc/s
1250 Mc/s
9380 Mc/s
1250 Mc/s
10 log10 (σ IN SQ METERS)
10 log10 (σ IN SQ METERS)
PERCENTAGE OF TIME THE VALUES EXCEED THE ORDINATE

Figure 6

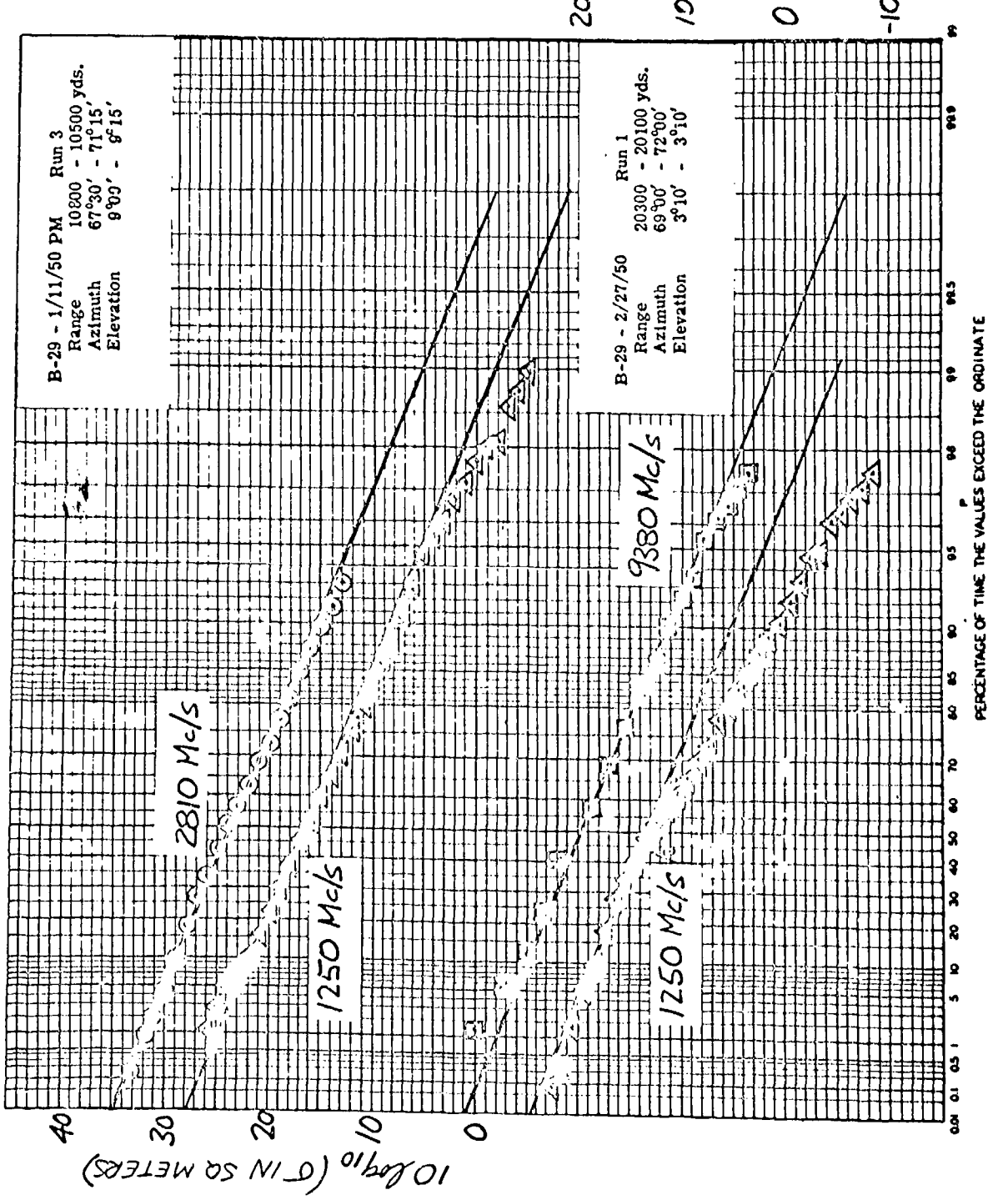
B-29 - 1/11/50 PM Run 3
Range 10800 - 10500 yds.
Azimuth 67°30' - 71°15'
Elevation 9°00' - 9°15'
B-29 - 2/27/50 Run 1
Range 20300 - 20100 yds.
Azimuth 69°00' - 72°00'
Elevation 3°10' - 3°10'
2810 Mc/s
1250 Mc/s
9380 Mc/s
1250 Mc/s
40 30 20 10 0
20 10 0 -10
10 log10 (σ IN SQ METERS)
10 log10 (σ IN SQ METERS)
PERCENTAGE OF TIME THE VALUES EXCEED THE ORDINATE
0.01 0.03 1 5 10 20 30 40 50 60 70 80 85 90 95 98 99

Figure 7

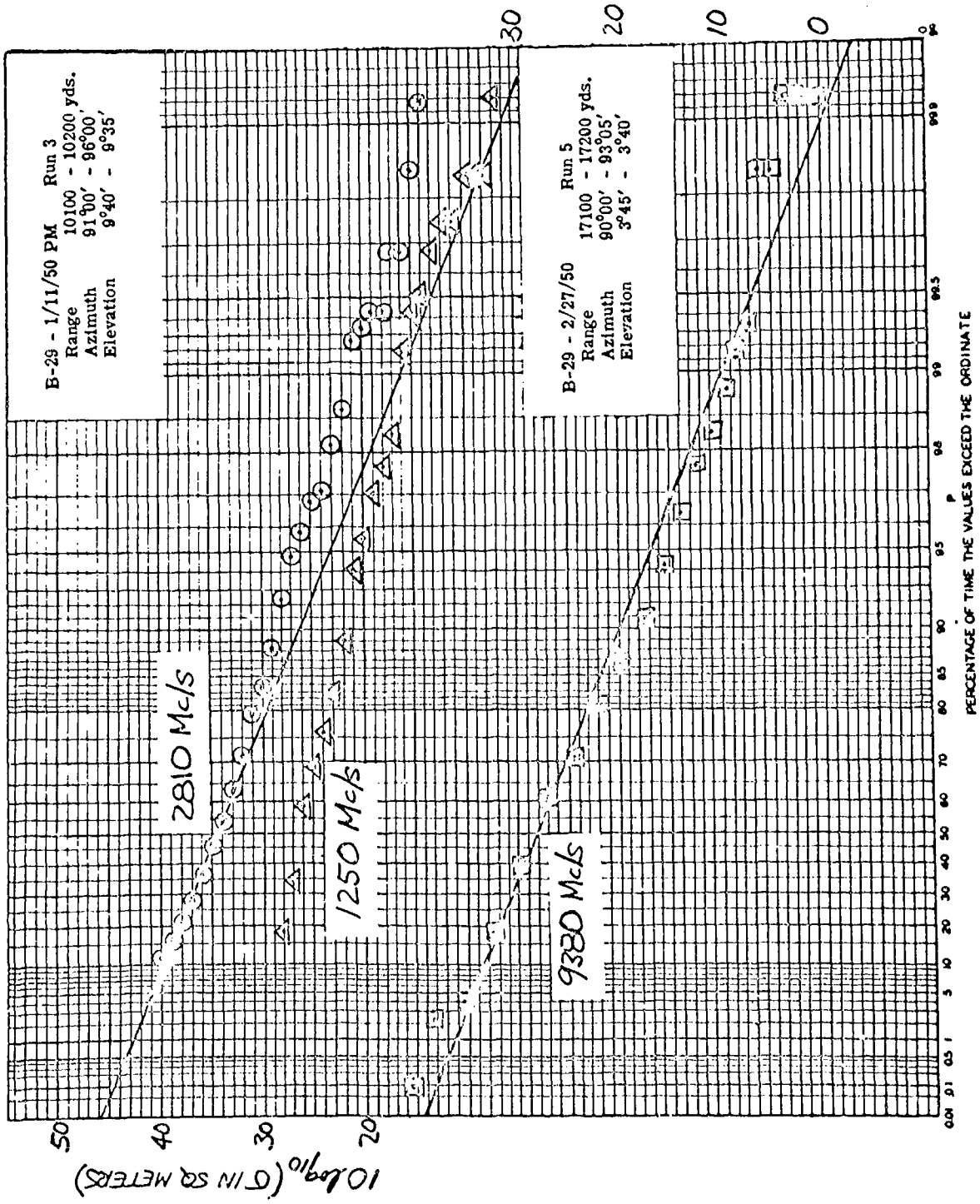
B-29 - 1/11/50 PM Run 3
Range 10100 - 10200 yds.
Azimuth 91°00′ - 96°00′
Elevation 9°40′ - 8°35′
B-29 - 2/27/50 Run 5
Range 17100 - 17200 yds.
Azimuth 90°00′ - 93°05′
Elevation 3°45′ - 3°40′
2810 M/s
1250 M/s
9380 M/s
10 log10 (G IN SQ METERS)
PERCENTAGE OF TIME THE VALUES EXCEED THE ORDINATE

Figure 8

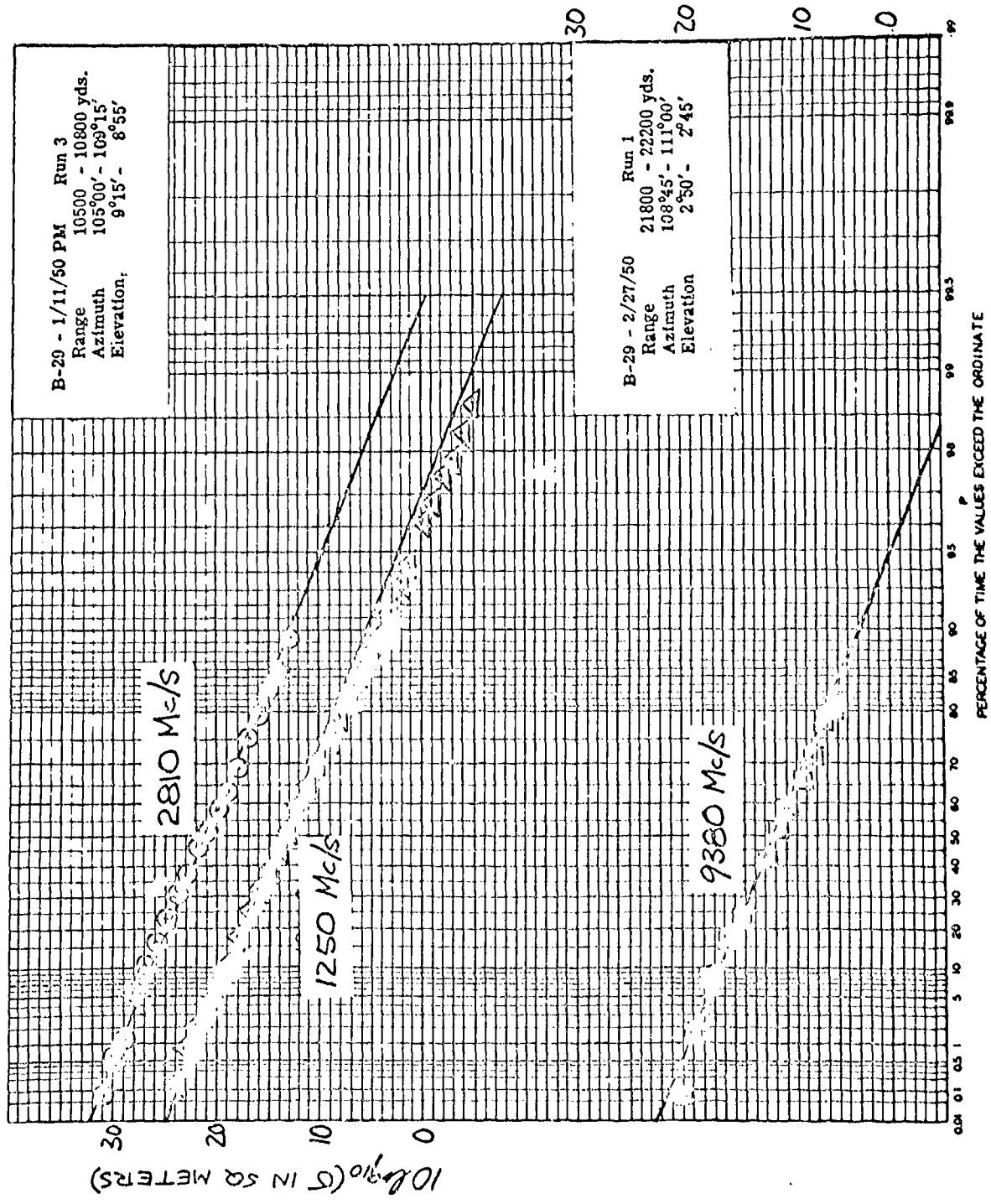
B-29 - 1/11/50 PM Run 3
Range 10500 - 10800 yds.
Azimuth 105°00' - 109°15'
Elevation 9°15' - 8°55'
B-29 - 2/27/50 Run 1
Range 21800 - 22200 yds.
Azimuth 108°45' - 111°00'
Elevation 2°50' - 2°45'
2810 Mc/s
1250 Mc/s
9380 Mc/s
30
20
10
0
log10 (σ IN SQ METERS)
PERCENTAGE OF TIME THE VALUES EXCEED THE ORDINATE

Figure 9

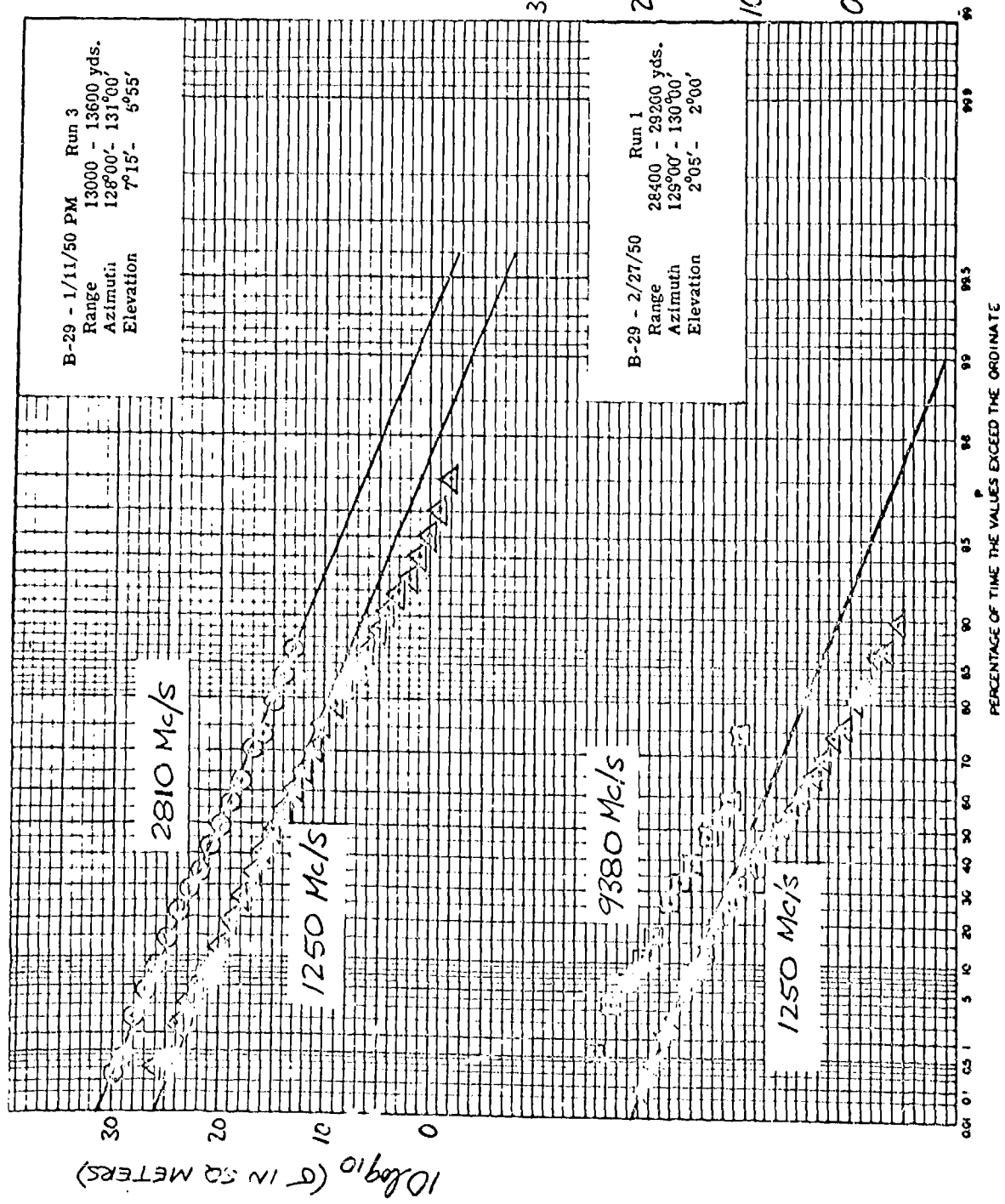
B-29 - 1/11/50 PM Run 3
Range 13000 - 13600 yds.
Azimuth 128°00′- 131°00′
Elevation 7°15′- 5°55′
B-29 - 2/27/50 Run 1
Range 28400 - 29200 yds.
Azimuth 129°00′- 130°00′
Elevation 2°05′- 2°00′
2810 Mc/s
1250 Mc/s
9380 Mc/s
1250 Mc/s
10 log10 (σ IN SQ METERS)
30
20
10
0
PERCENTAGE OF TIME THE VALUES EXCEED THE ORDINATE

Figure 10

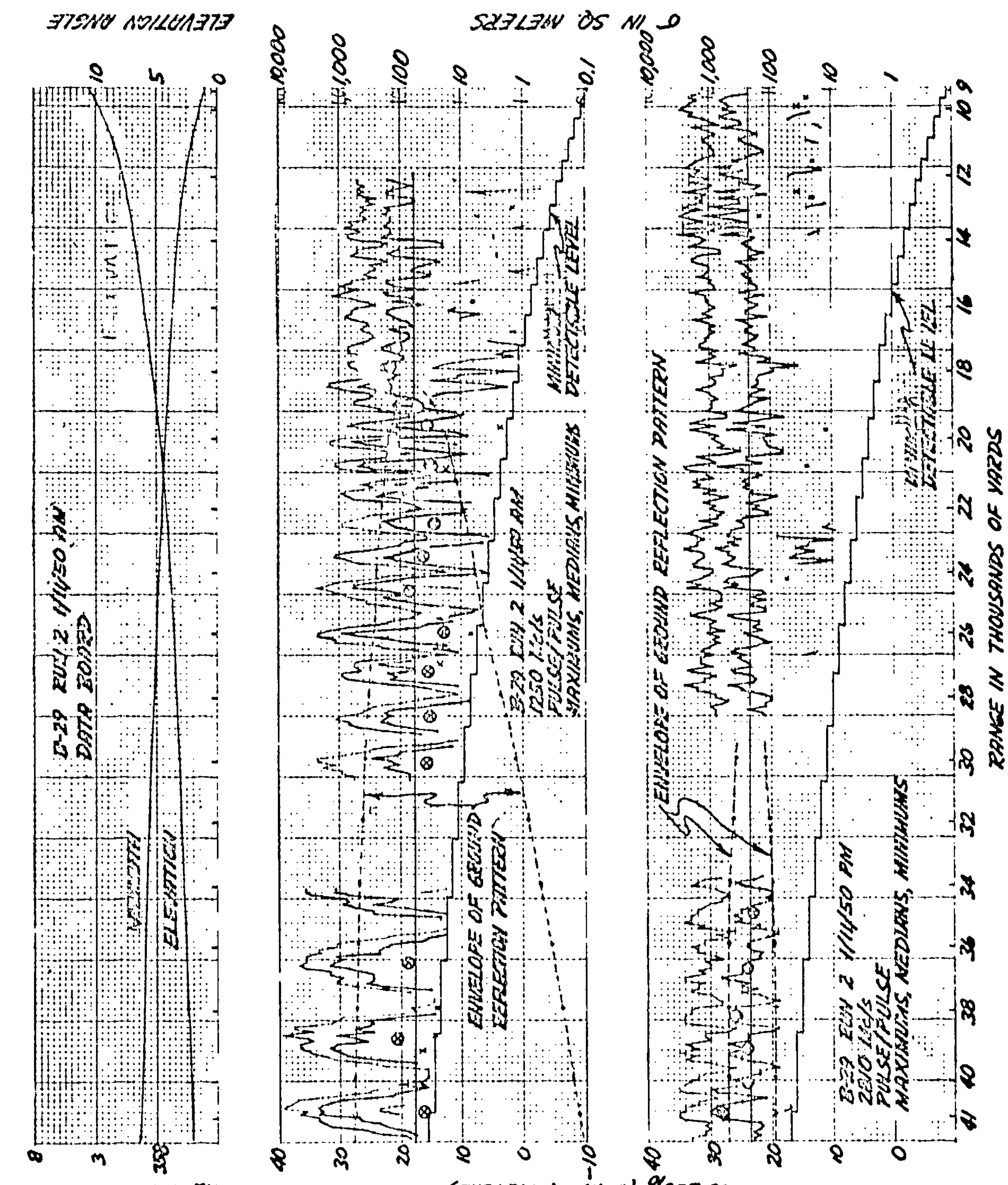
ELEVATION ANGLE
AZIMUTH ANGLE
B-29 RUN 2 1/14/50 PM
DATA BOARD
ELEVATION
σ IN SQ. METERS
10 LOG10 (σ IN SQ. METERS)
ENVELOPE OF GROUND REFLECTION PATTERN
MINIMUM DETECTABLE LEVEL
B-29 RUN 2 1/14/50 AM
PULSE/PULSE
MAXIMUMS, MEDIANS, MINIMUMS
B-29 RUN 2 1/14/50 PM
PULSE/PULSE
MAXIMUMS, MEDIANS, MINIMUMS
RANGE IN THOUSANDS OF YARDS

Figure 11

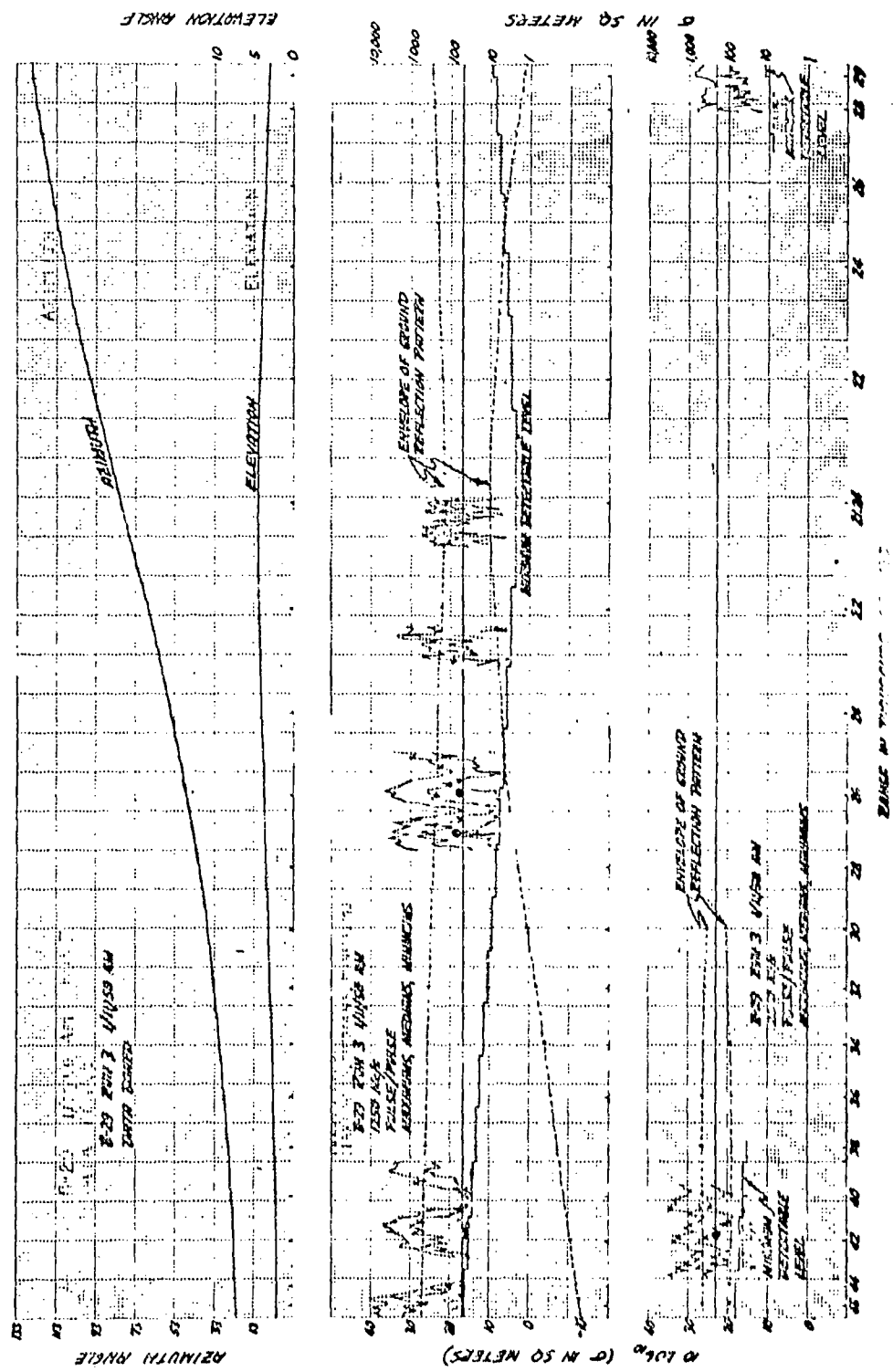
ELEVATION ANGLE
ELEVATION
AZIMUTH ANGLE
AZIMUTH
σ IN SQ METERS
ENVELOPE OF ECHO REFLECTION PATTERN
RANGE RESOLUTION LIMIT
RANGE IN YARDS

Figure 12

CONFIDENTIAL

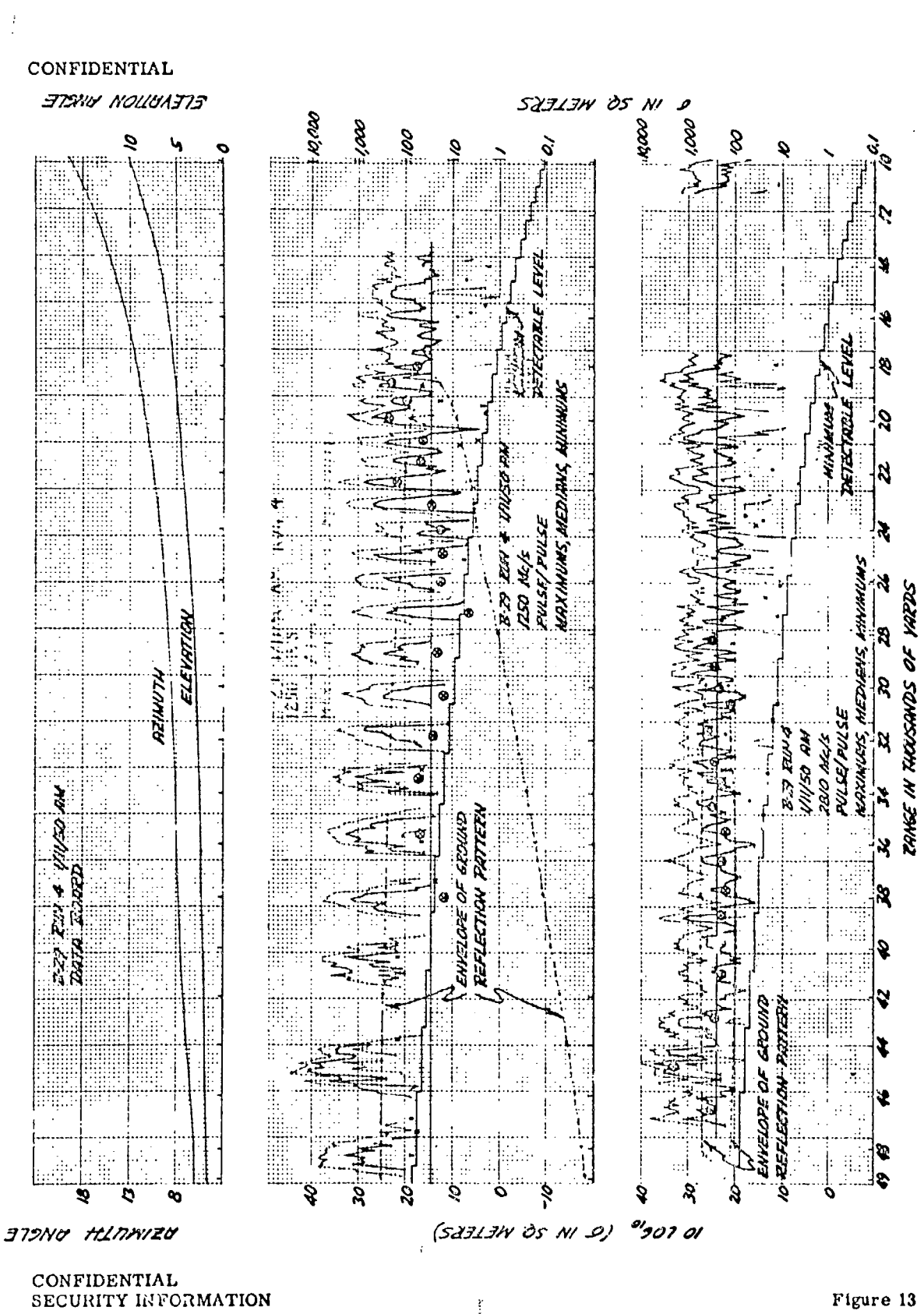

CONFIDENTIAL
SECURITY INFORMATION

Figure 13

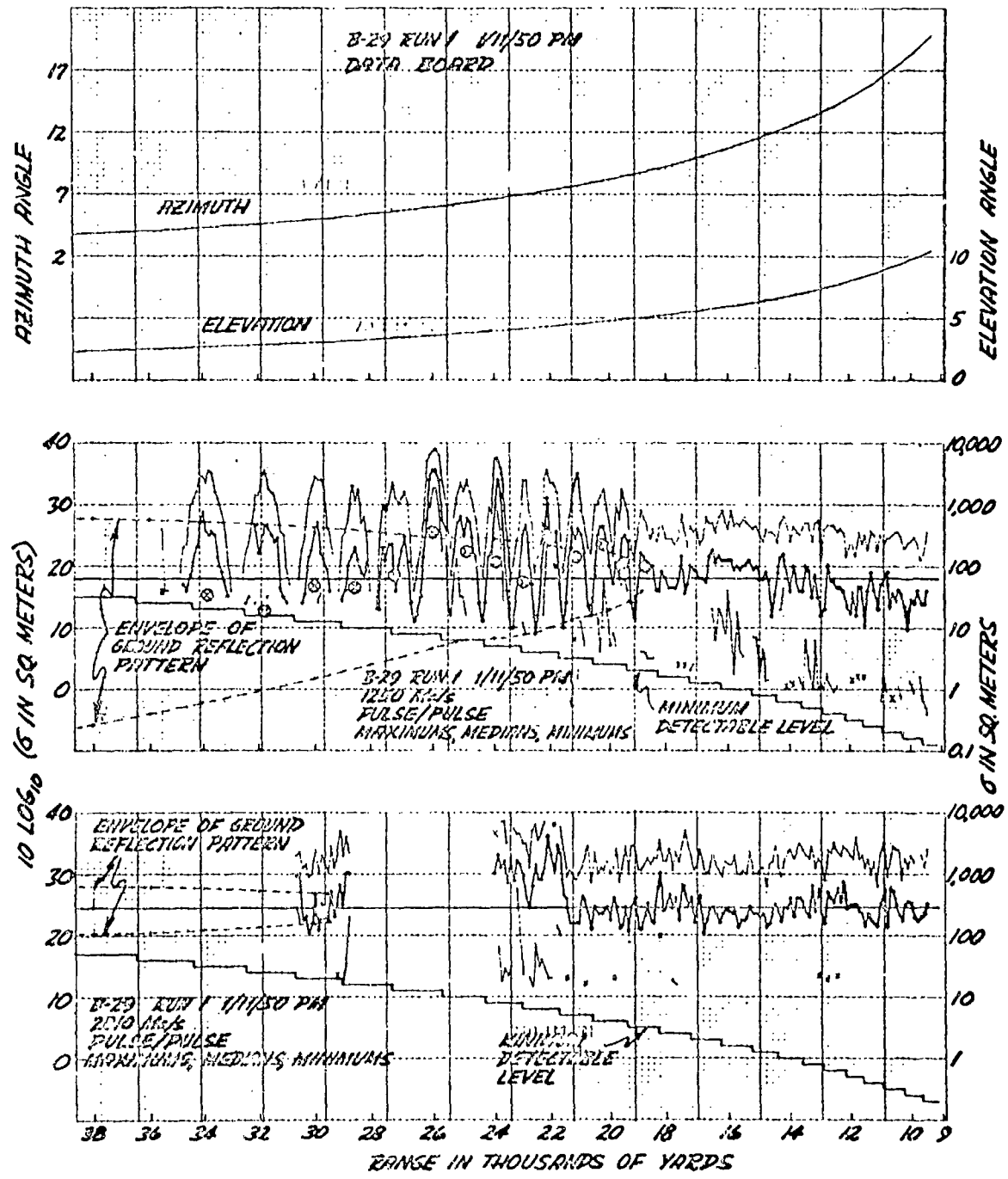
B-29 RUN 1 1/11/50 PM
DATA BOARD
AZIMUTH
ELEVATION
AZIMUTH ANGLE
ELEVATION ANGLE
17
12
7
2
10
5
0
ENVELOPE OF GROUND REFLECTION PATTERN
B-29 RUN 1 1/11/50 PM
1250 RPS
PULSE/PULSE
MAXIMUMS, MEDIUMS, MINIMUMS
MINIMUM DETECTABLE LEVEL
10 LOG10 (σ IN SQ METERS)
σ IN SQ METERS
40
30
20
10
0
10,000
1,000
100
10
1
0.1
ENVELOPE OF GROUND REFLECTION PATTERN
B-29 RUN 1 1/11/50 PM
2010 RPS
PULSE/PULSE
MAXIMUMS, MEDIUMS, MINIMUMS
MINIMUM DETECTABLE LEVEL
38 36 34 32 30 28 26 24 22 20 18 16 14 12 10 9
RANGE IN THOUSANDS OF YARDS

Figure 14

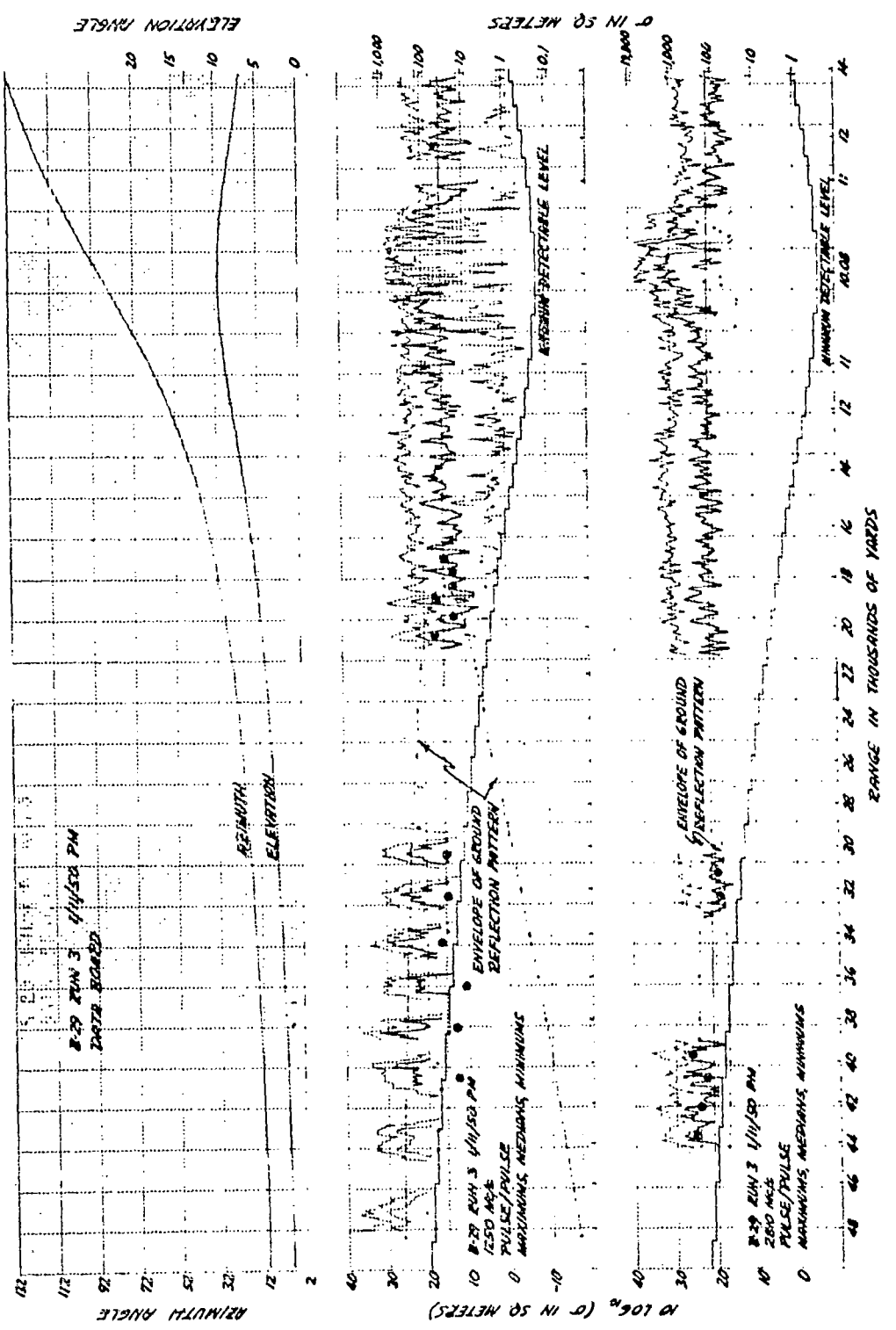
AZIMUTH ANGLE
ELEVATION ANGLE
AZIMUTH
ELEVATION
B-29 RUN 3 1/11/50 PM
DATA BOARD
N LOG10 (σ IN SQ METERS)
σ IN SQ METERS
ENVELOPE OF GROUND REFLECTION PATTERN
MINIMUM DETECTABLE LEVEL
B-29 RUN 3 1/11/50 PM
1250 MCS
PULSE/PULSE
MAXIMUMS, MEDIANS, MINIMUMS
B-29 RUN 3 1/11/50 PM
2810 MCS
PULSE/PULSE
MAXIMUMS, MEDIANS, MINIMUMS
RANGE IN THOUSANDS OF YARDS

Figure 15

CONFIDENTIAL

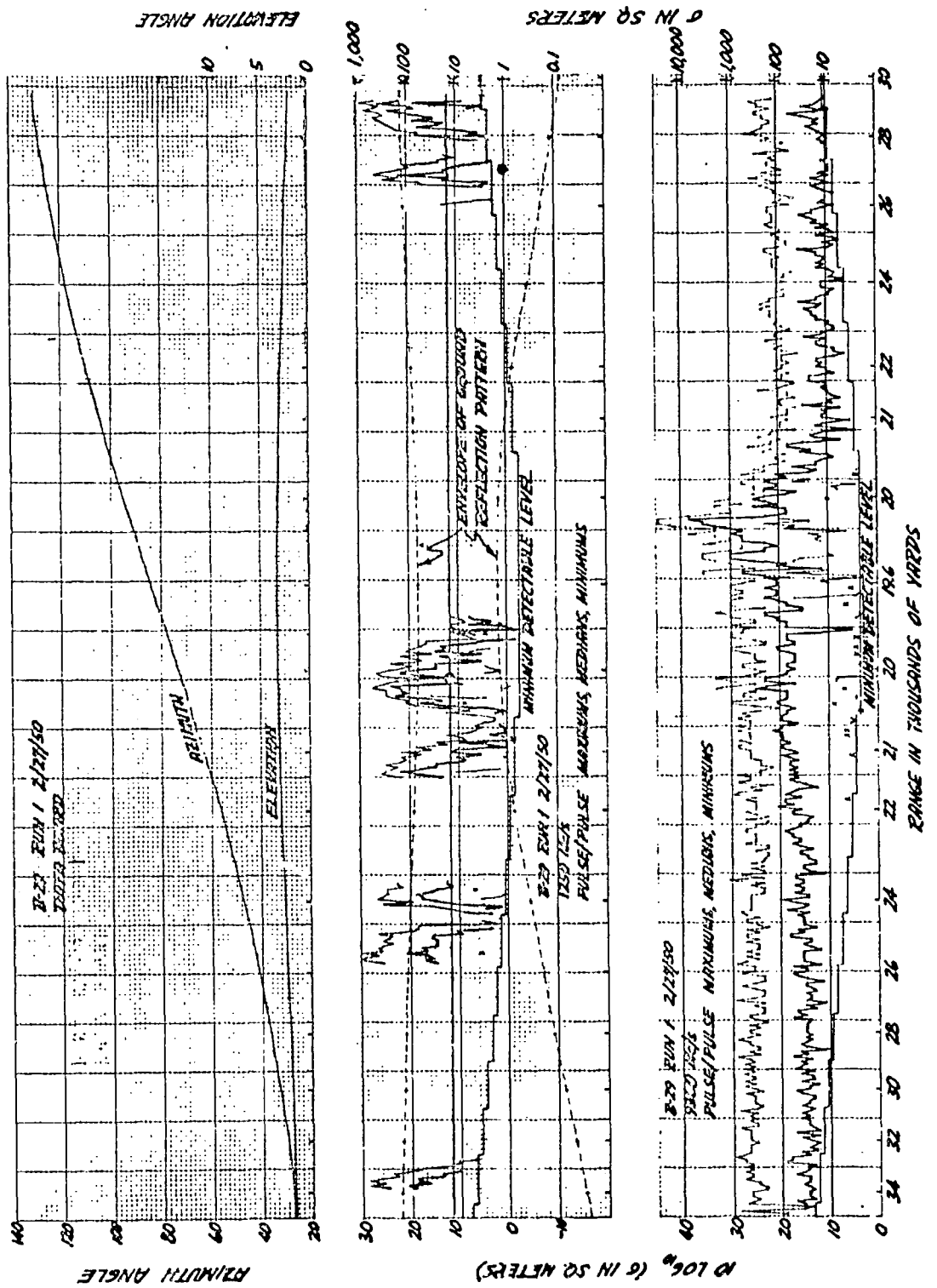

CONFIDENTIAL
SECURITY INFORMATION

Figure 16

CONFIDENTIAL

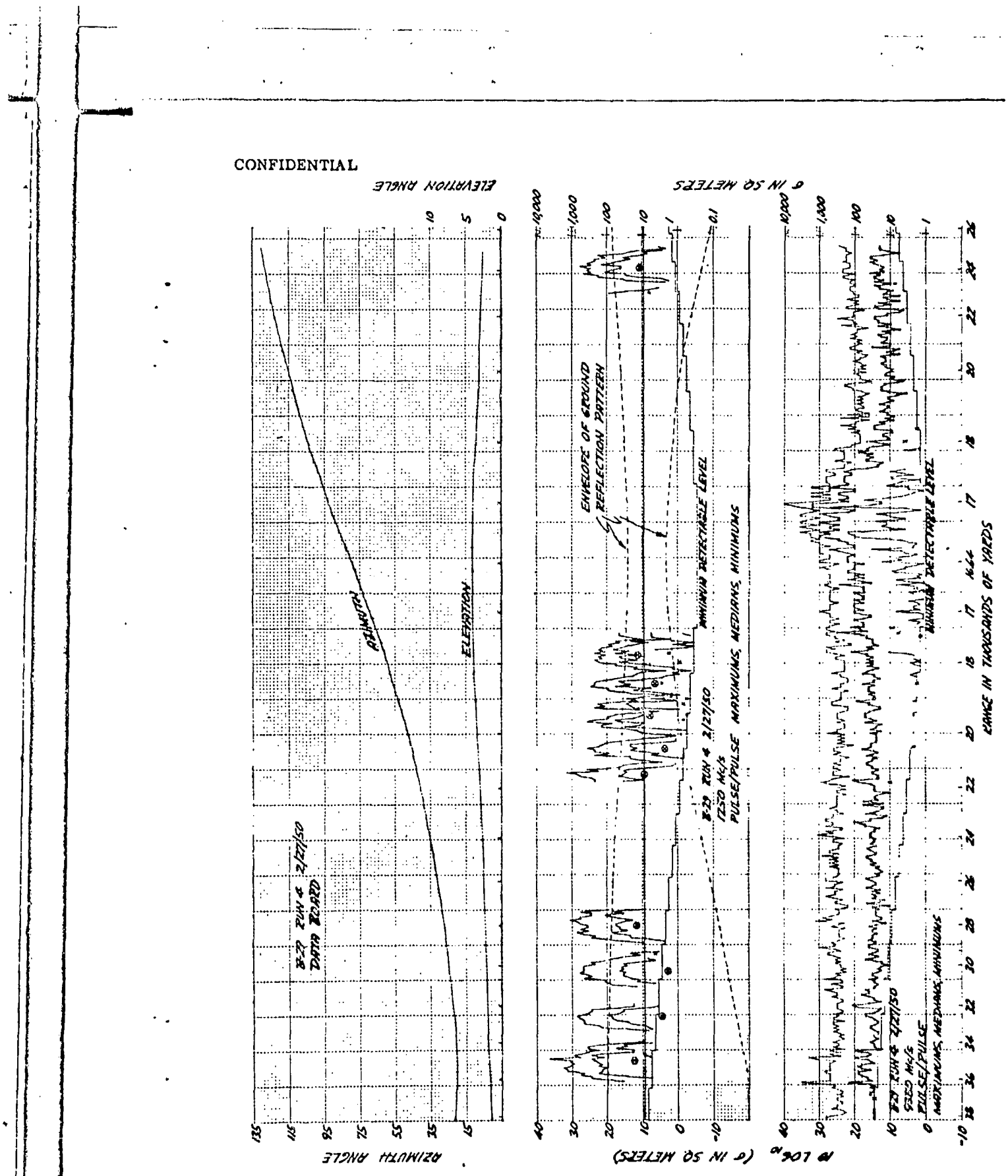

CONFIDENTIAL
SECURITY INFORMATION

Figure 17

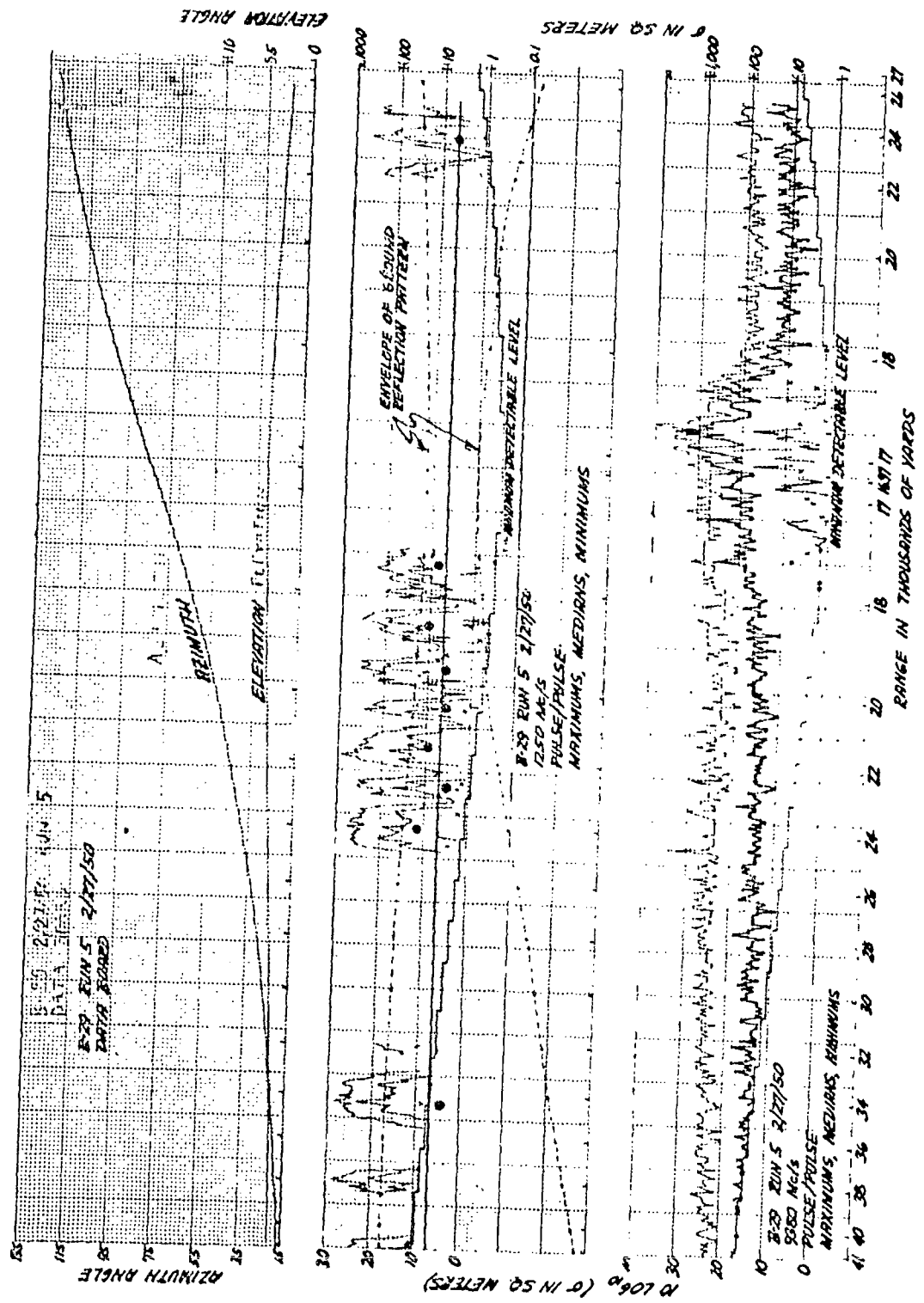

CONFIDENTIAL
SECURITY INFORMATION

Figure 18

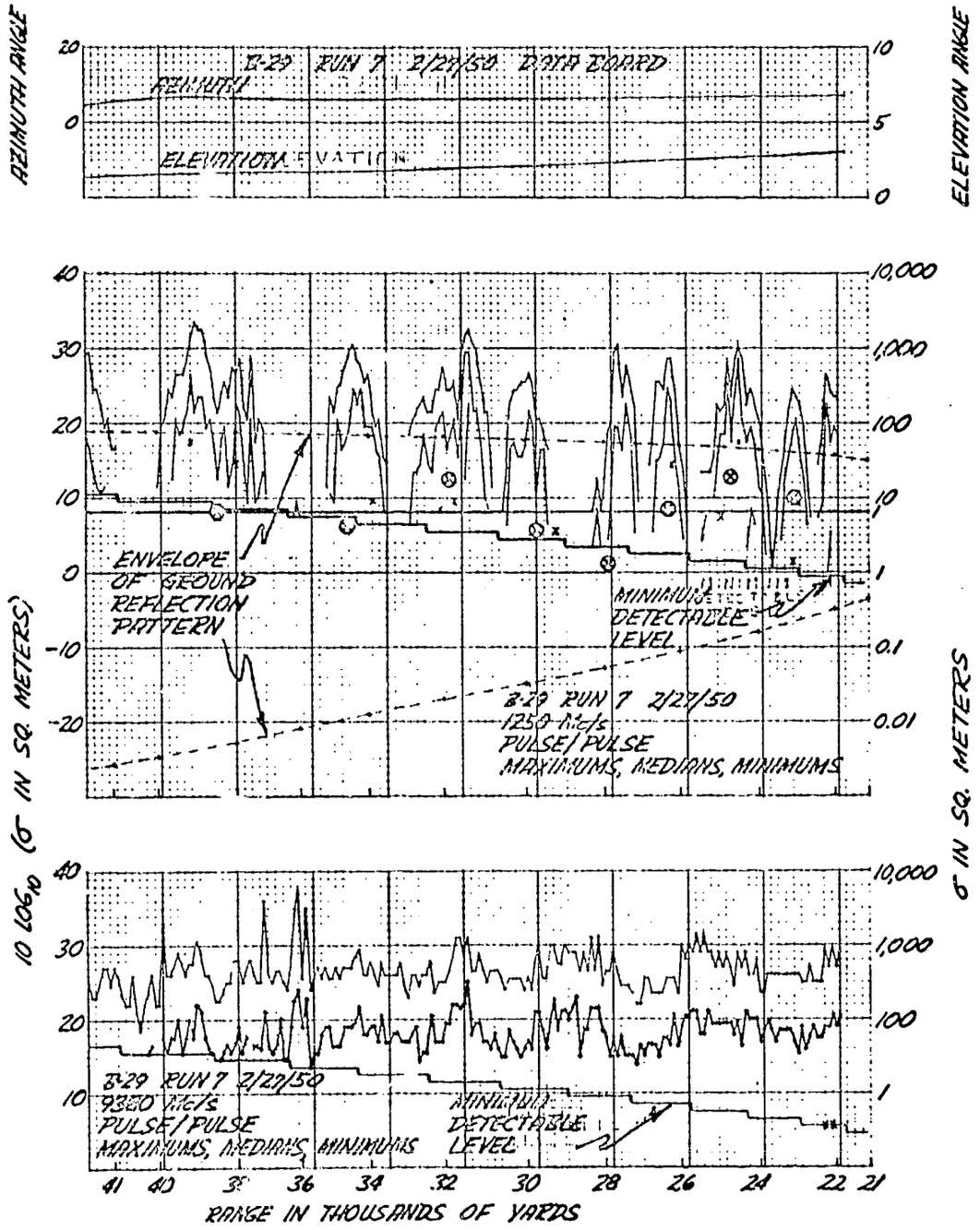
AZIMUTH ANGLE
ELEVATION ANGLE
E-29 RUN 7 2/27/50 DATA BOARD
AZIMUTH
ELEVATION
20
0
10
5
0
40
30
20
10
0
-10
-20
10,000
1,000
100
10
1
0.1
0.01
ENVELOPE OF GROUND REFLECTION PATTERN
MINIMUMS DETECTABLE LEVEL
E-29 RUN 7 2/27/50
1250 Mc/s
PULSE/PULSE
MAXIMUMS, MEDIANS, MINIMUMS
10 LOG10 (σ IN SQ. METERS)
σ IN SQ. METERS
E-29 RUN 7 2/27/50
9380 Mc/s
PULSE/PULSE
MAXIMUMS, MEDIANS, MINIMUMS
MINIMUMS DETECTABLE LEVEL
41 40 38 36 34 32 30 28 26 24 22 21
RANGE IN THOUSANDS OF YARDS

Figure 19

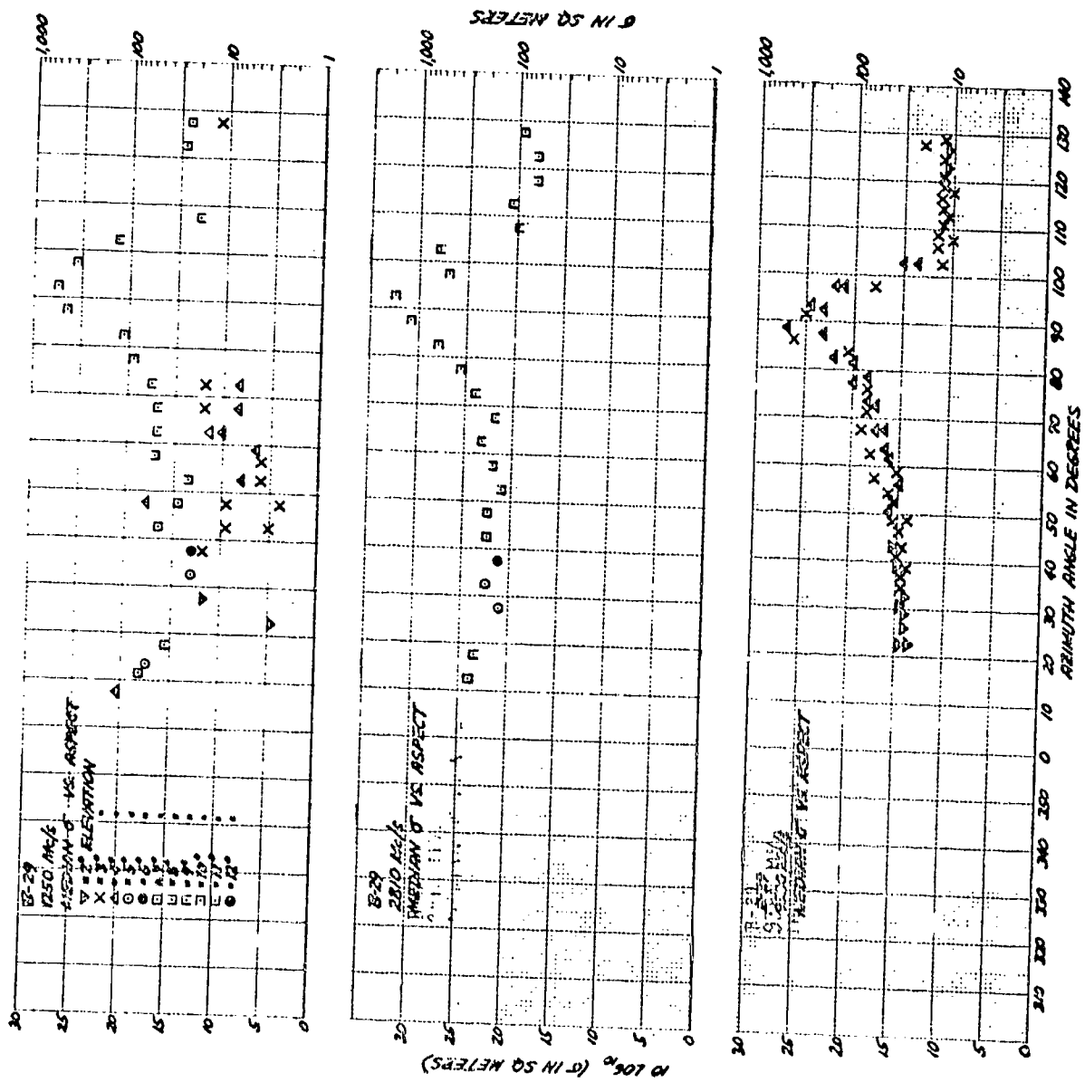
B-29
1250 Mc/s
MEDIAN σ VS. ASPECT
ELEVATION
B-29
2810 Mc/s
MEDIAN σ VS. ASPECT
B-29
9375 Mc/s
MEDIAN σ VS. ASPECT
σ IN SQ METERS
10 log10 (σ IN SQ METERS)
AZIMUTH ANGLE IN DEGREES

Figure 20

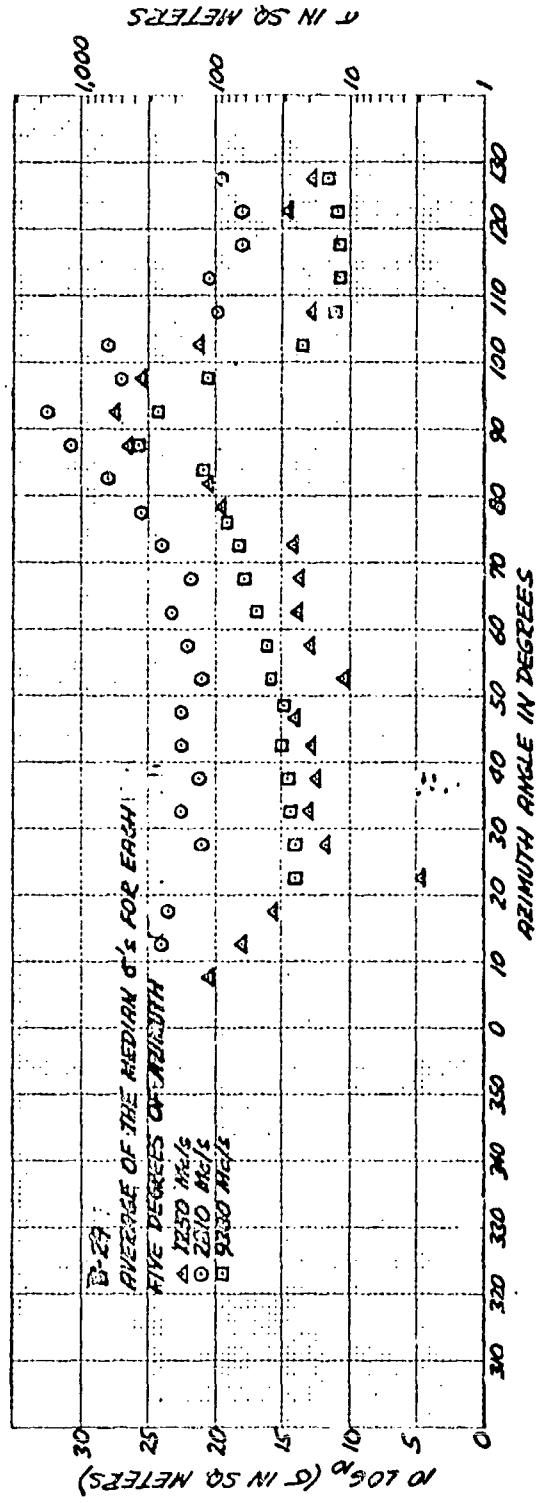
σ IN SQ METERS
1,000
100
10
1
130
120
110
100
90
80
70
60
50
40
30
20
10
0
350
340
330
320
310
AZIMUTH ANGLE IN DEGREES
30
25
20
15
10
5
0
log10 (σ IN SQ METERS)
B-29
AVERAGE OF THE MEDIAN σ's FOR EACH FIVE DEGREES OF AZIMUTH
1250 Mc/s
2010 Mc/s
9230 Mc/s

Figure 21

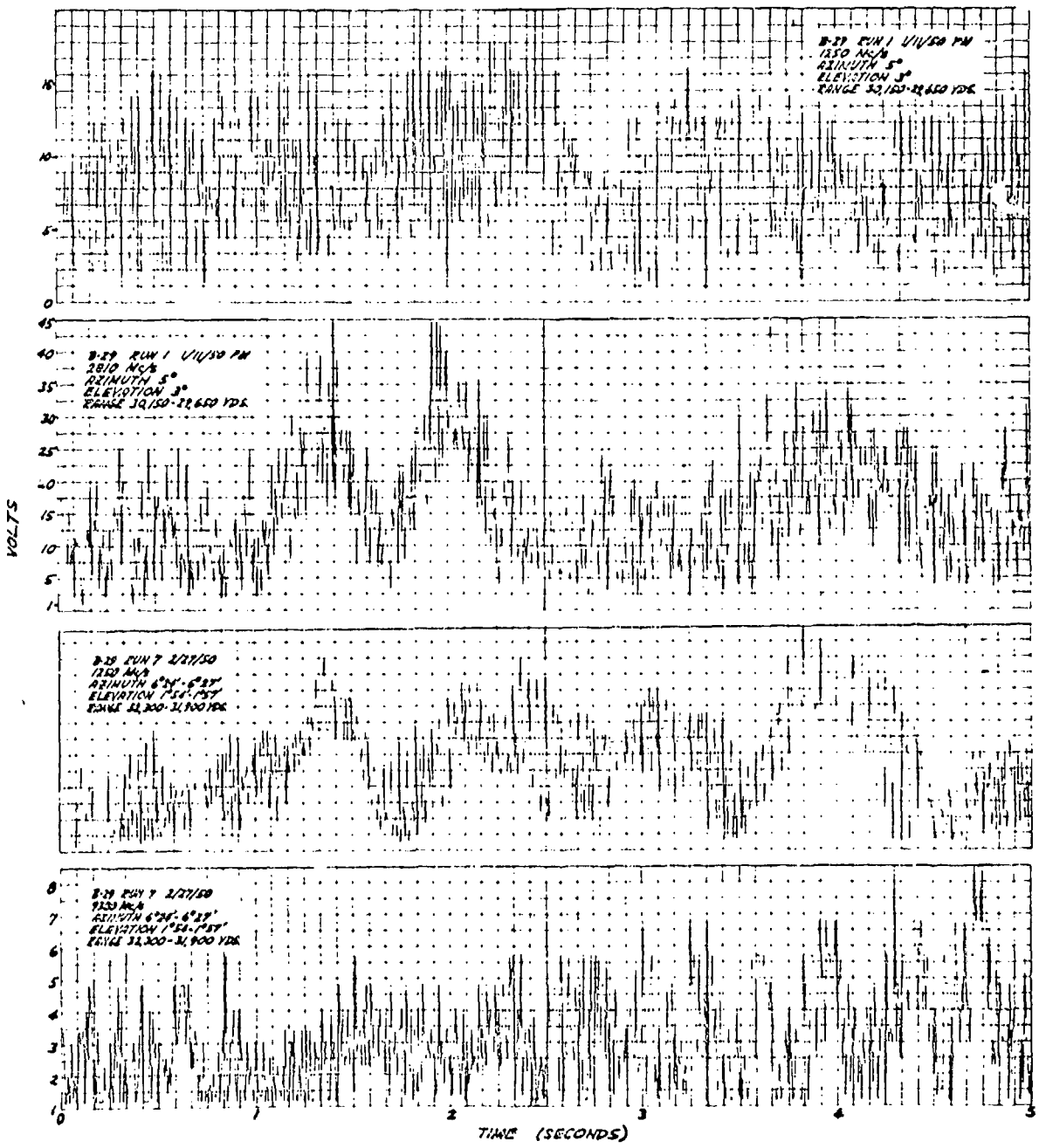

CONFIDENTIAL
SECURITY INFORMATION

Figure 22

CONFIDENTIAL

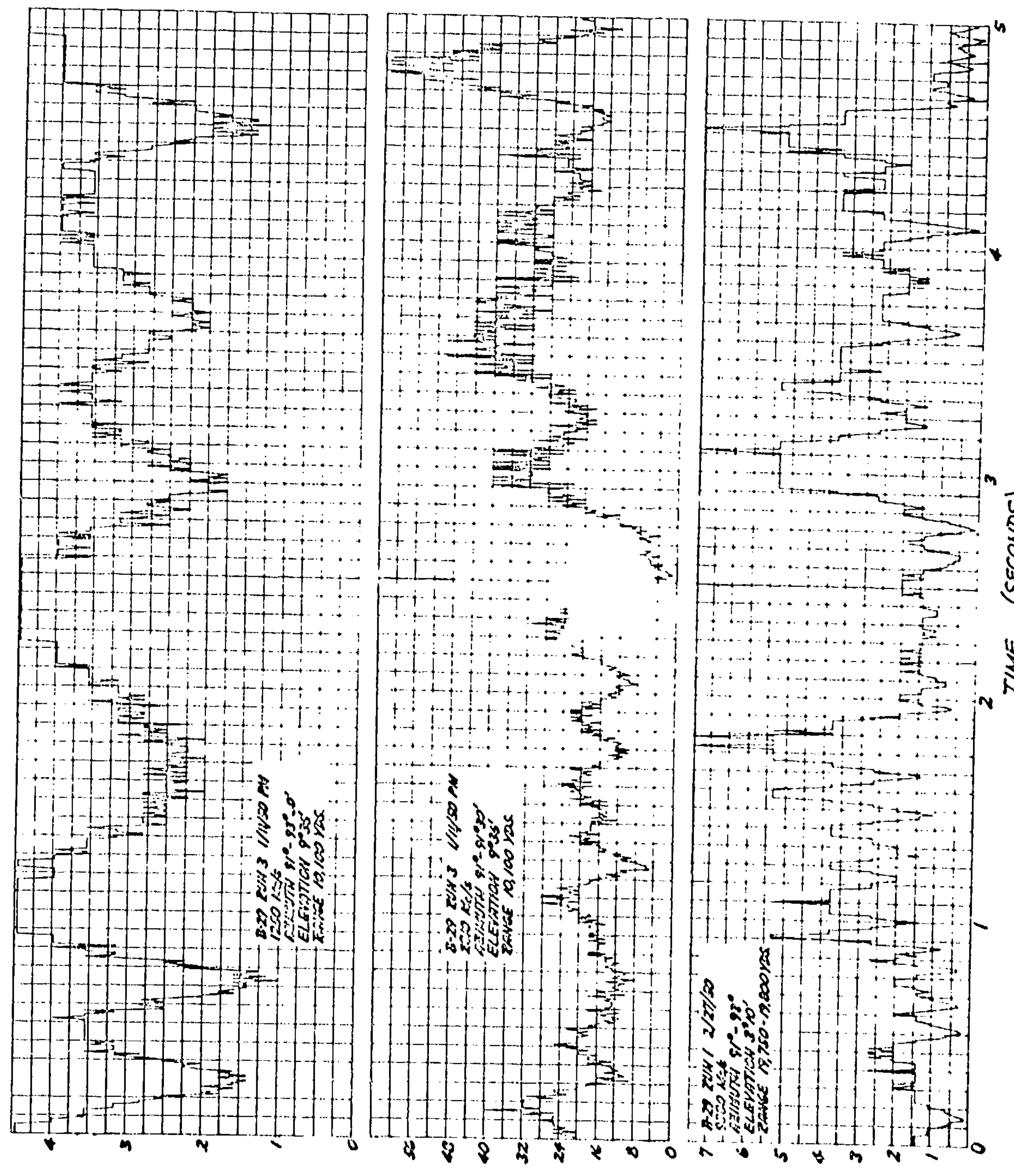

CONFIDENTIAL
SECURITY INFORMATION

Figure 23

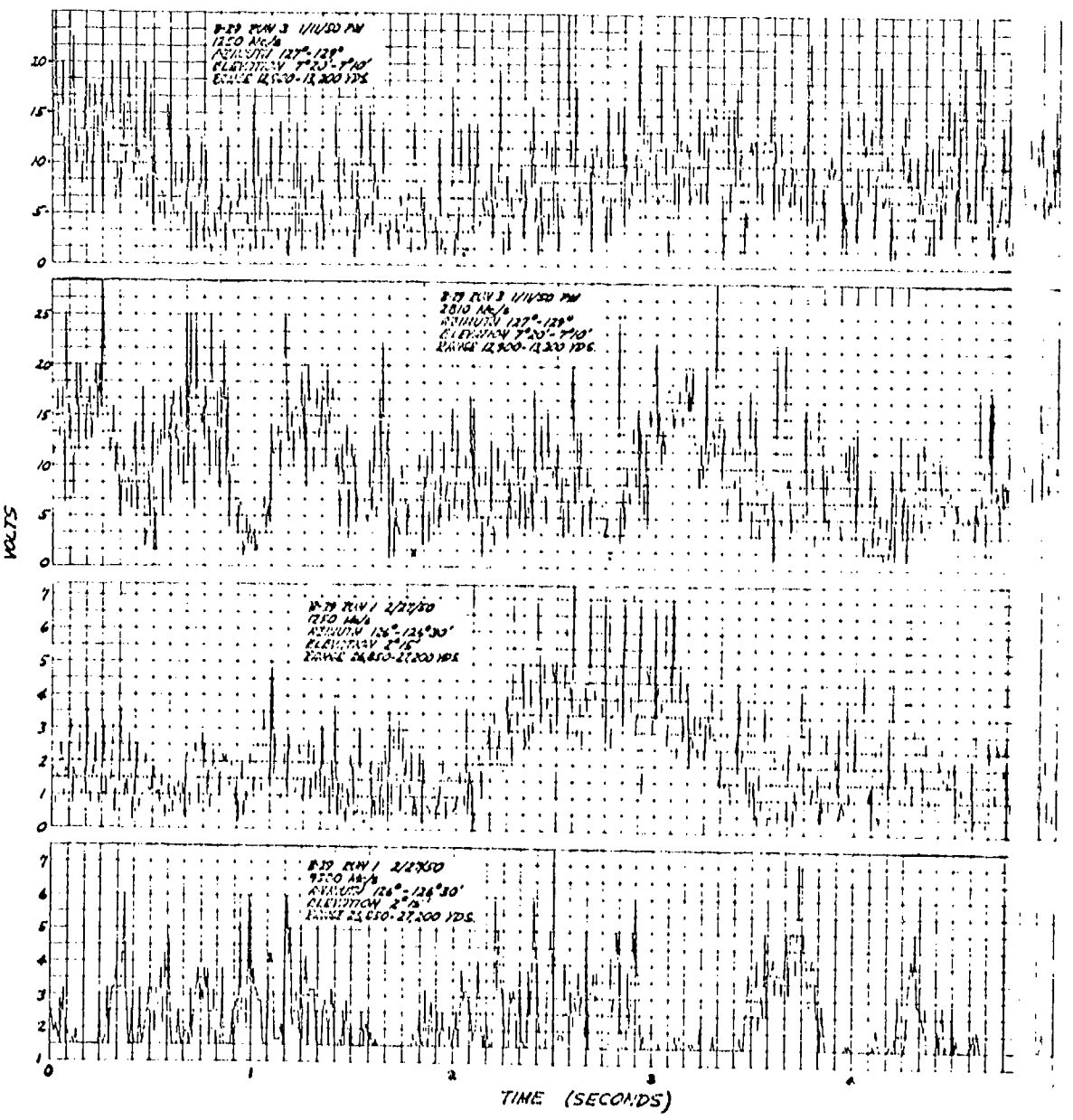

Figu

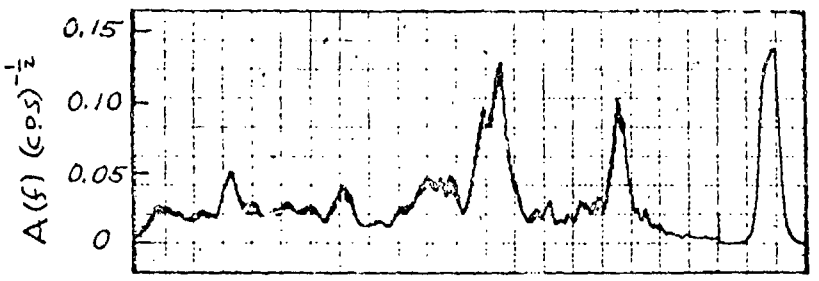

B-29 Run 1
1250 Mc/s
Azimuth 5°
Elevation 3°
Range 30,150 - 29650 yds.

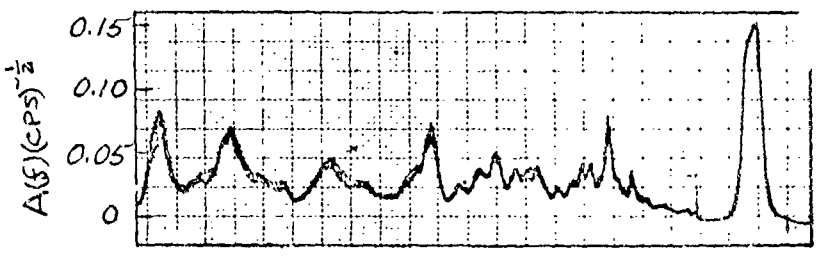

B-29 Run 1
2810 Mc/s
Azimuth 5°
Elevation 3°
Range 30,150 - 29,650 yds.

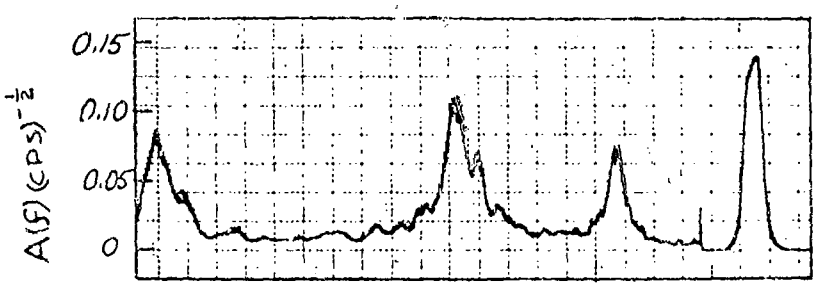

B-29 Run 7
1250 Mc/s
Azimuth 6°24' - 6°27'
Elevation 1°54' - 1°57'
Range 32,300 - 31,900

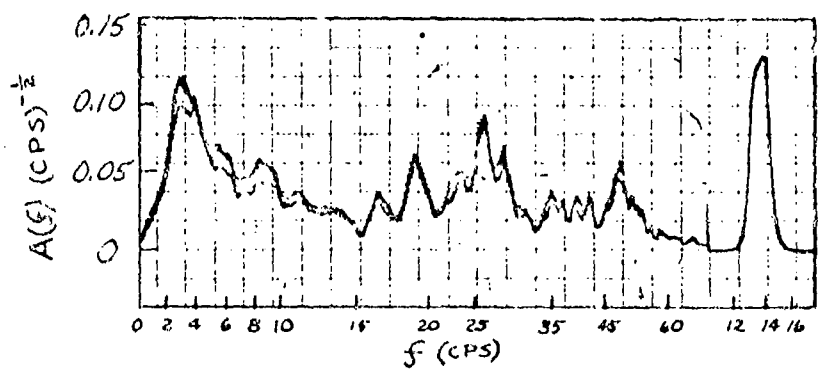

B-29 Run 7
9380 Mc/s
Azimuth 6°24'-6°27'
Elevation 1°54' - 1°57'
Range 32,300 - 31,900

Figure 25

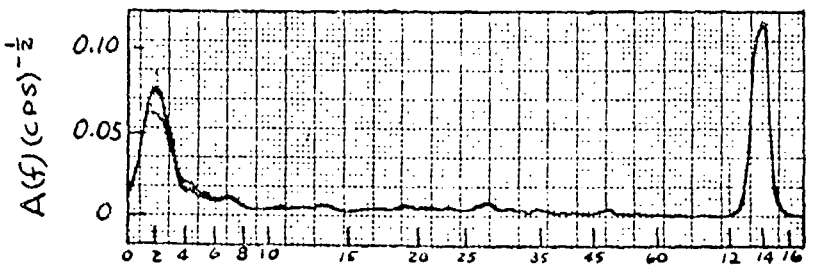

B-29 Run 3
1250 Mc/s
Azimuth 91°-93°30'
Elevation 9°36'
Range 10,100 yds.

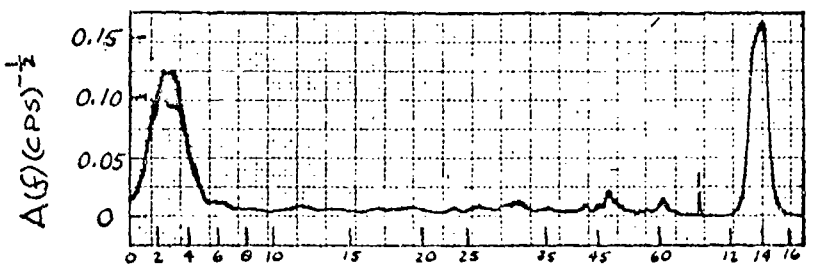

B-29 Run 3
2810 Mc/s
Azimuth 91°-93°30'
Elevation 9°36'
Range 10,100 yds.

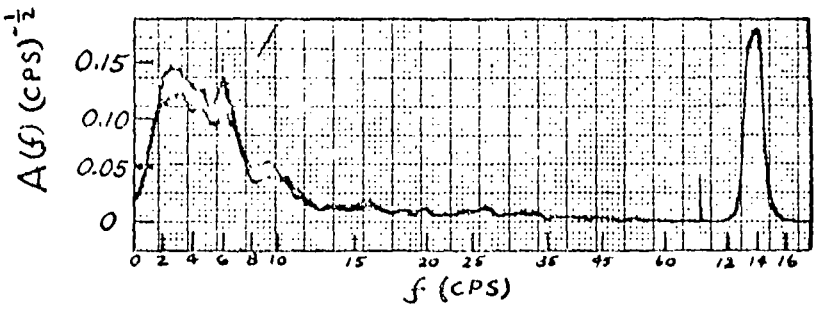

B-29 Run 1
9380 Mc/s
Azimuth 91°-93°
Elevation 3°10'
Range 19,750-19,800 yds.

Figure 26

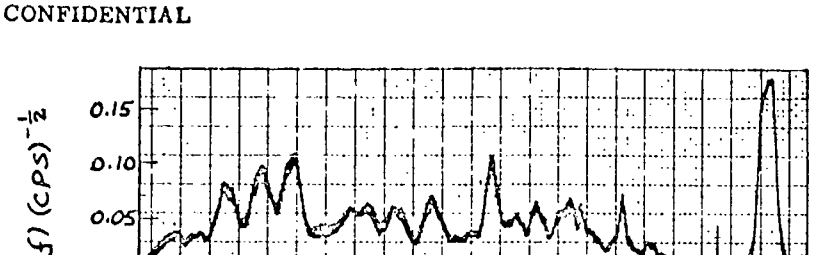

B-29 Run 3
1250 Mc/s
Azimuth 127°-129°
Elevation 7°20' -7°10'
Range 12,900-13,200 yds.

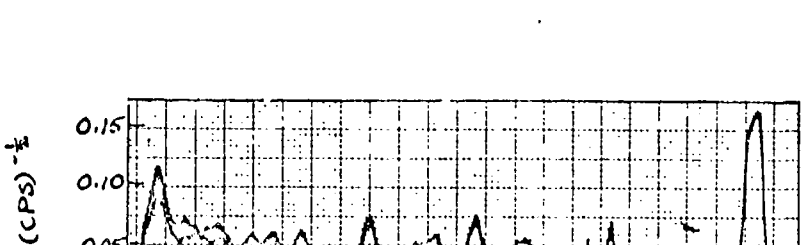

B-29 Run 3
2810 Mc/s
Azimuth 127°-129°
Elevation 7°20' -7°10'
Range 12,900-13,200 yds.

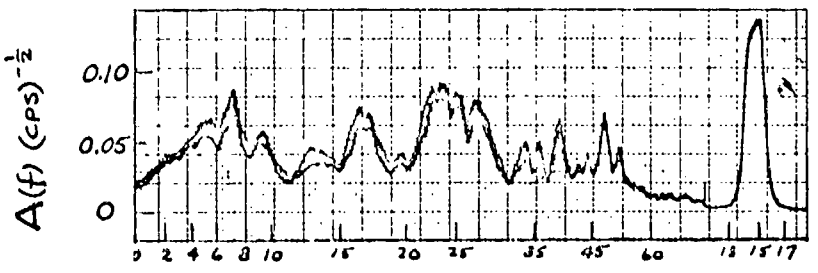

B-29 Run 1
1250 Mc/s
Azimuth 126°-126°30'
Elevation 2°15'
Range 26,850-27,200 yds.

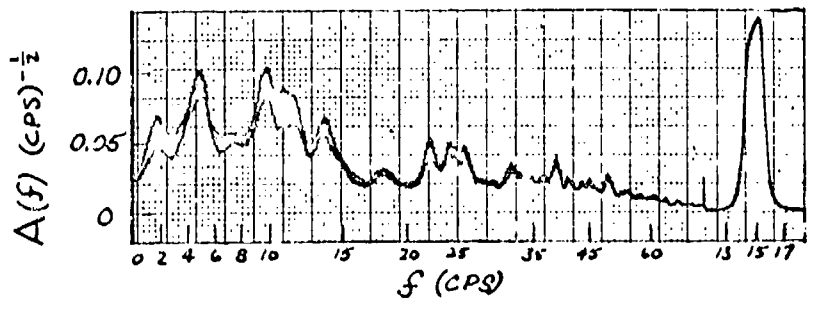

B-29 Run 1
9380 Mc/s
Azimuth 126°-126°30'
Elevation 2°15'
Range 26,850-27,200 yds.

Figure 27

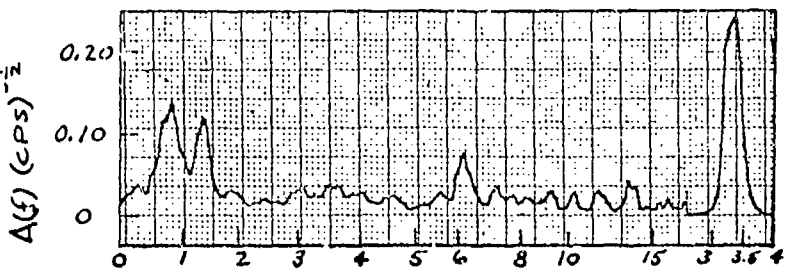

B-29 Run 1
1250 Mc/s
Azimuth 5°
Elevation 3°
Range 30,150-29,650 yds.

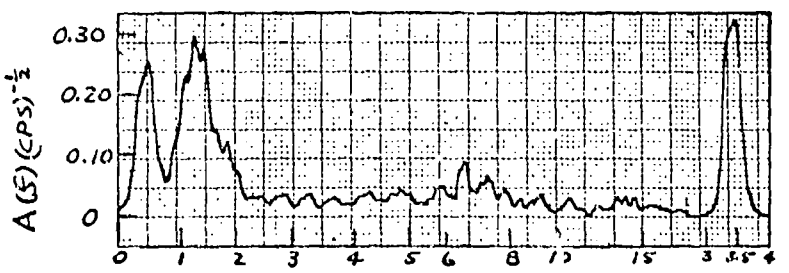

B-29 Run 1
2810 Mc/s
Azimuth 5°
Elevation 3°
Range 30,150-29,650 yds.

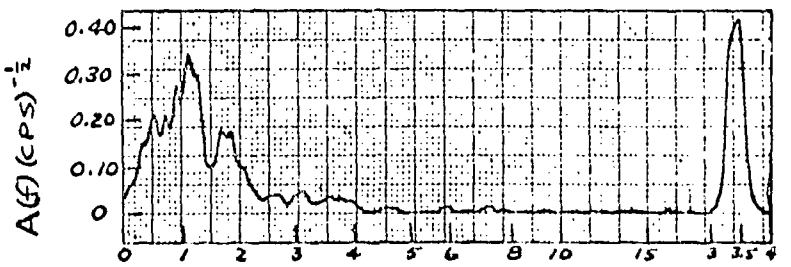

B-29 Run 7
1250 Mc/s
Azimuth 6°24'-6°27'
Elevation 1°54'-1°57'
Range 32,300-31,900 yds.

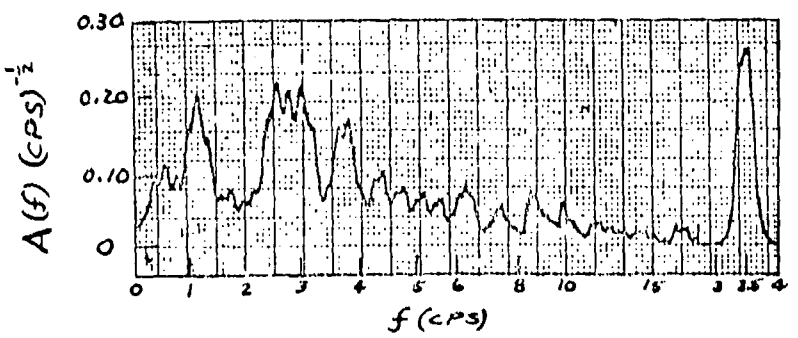

B-29 Run 7
9380 Mc/s
Azimuth 6°24'-6°27'
Elevation 1°54'-1°57'
Range 32,300-31,900 yds.

SECURITY INFORMATION

Figure 28

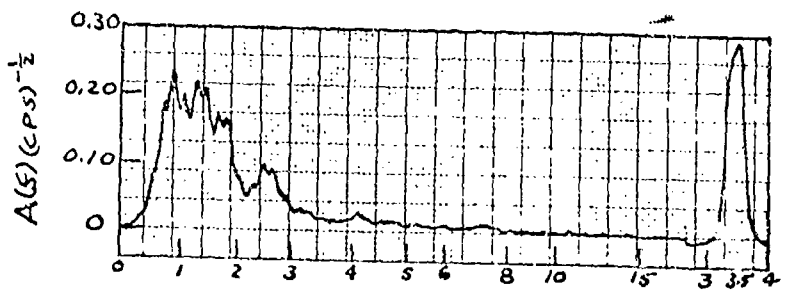

B-29 Run 3
1250 Mc/s
Azimuth 91°-93°30'
Elevation 9°36'
Range 10,100 yds

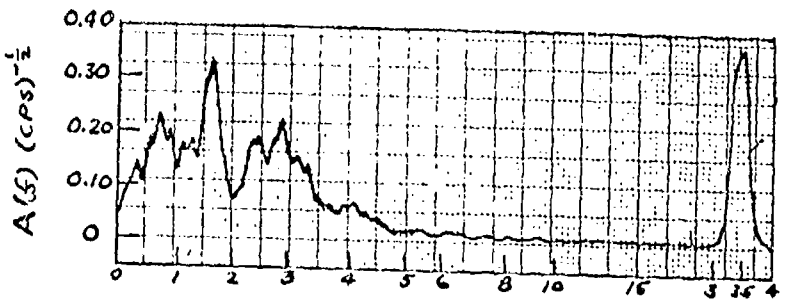

B-29 Run 3
2810 Mc/s
Azimuth 91°-93°30'
Elevation 9°36'
Range 10,100 yds.

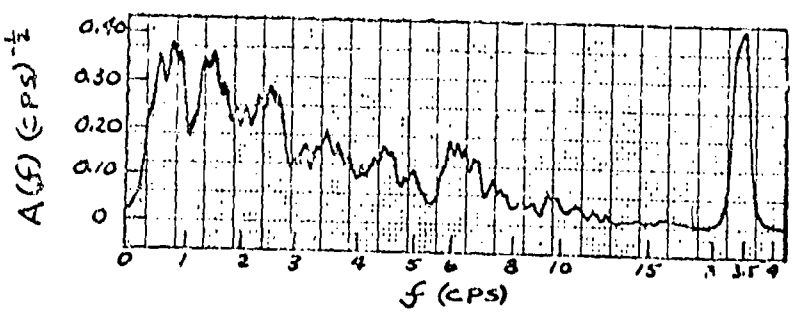

B-29 Run 1
9380 Mc/s
Azimuth 91°-93°
Elevation 3°10'
Range 19,750-19,800 yds

[redacted]
SECURITY INFORMATION

Figure 29

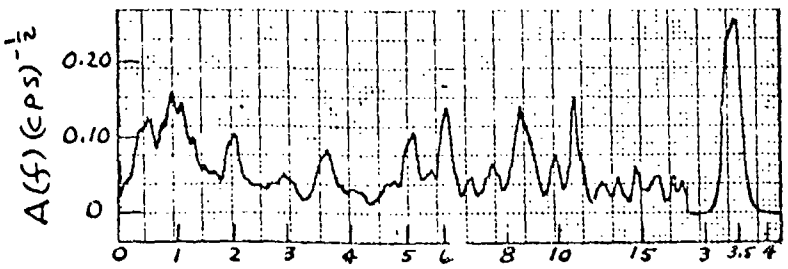

B-29 Run 3
1250 Mc/s
Azimuth 127°-129°
Elevation 7°20'-7°10'
Range 12,900-13,200 yds

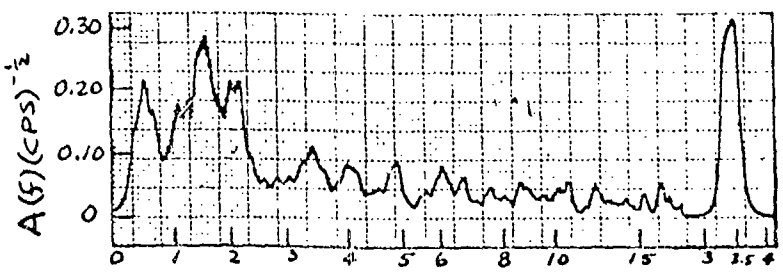

B-29 Run 3
2810 Mc/s
Azimuth 127°-129°
Elevation 7°20'-7°10'
Range 12,900-13,200 yds

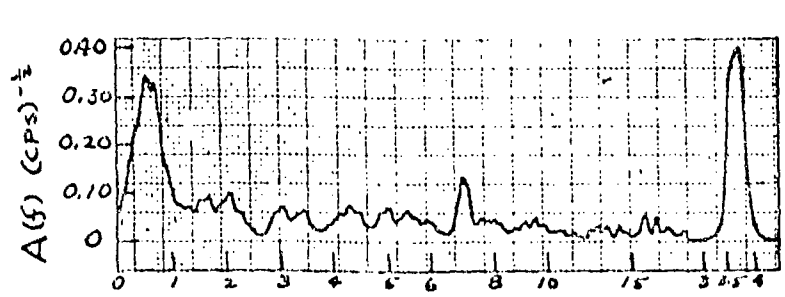

B-29 Run 1
1250 Mc/s
Azimuth 126°-126°30'
Elevation 2°15'
Range 26,850-27,200 yds

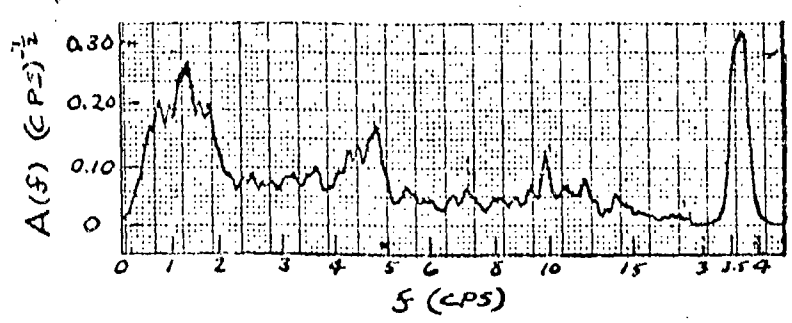

B-29 Run 1
9380 Mc/s
Azimuth 126°-126°30'
Elevation 2°15'
Range 26,850-27,200 yds

SECURITY INFORMATION

Figure 30